ISSCC 2019

SESSION 29

Quantum & Photonics Technologies

A Scalable Quantum Magnetometer in 65nm CMOS with Vector-Field Detection Capability

Mohamed I. Ibrahim, Christopher Foy,
Dirk R. Englund, and Ruonan Han

Massachusetts Institute of Technology
Cambridge, MA, USA

© 2019 IEEE

Applications of Magnetometers

- Magnetic field sensors are used for navigation, tracking, mineral exploration, current sensing, magnetocardiography and other applications

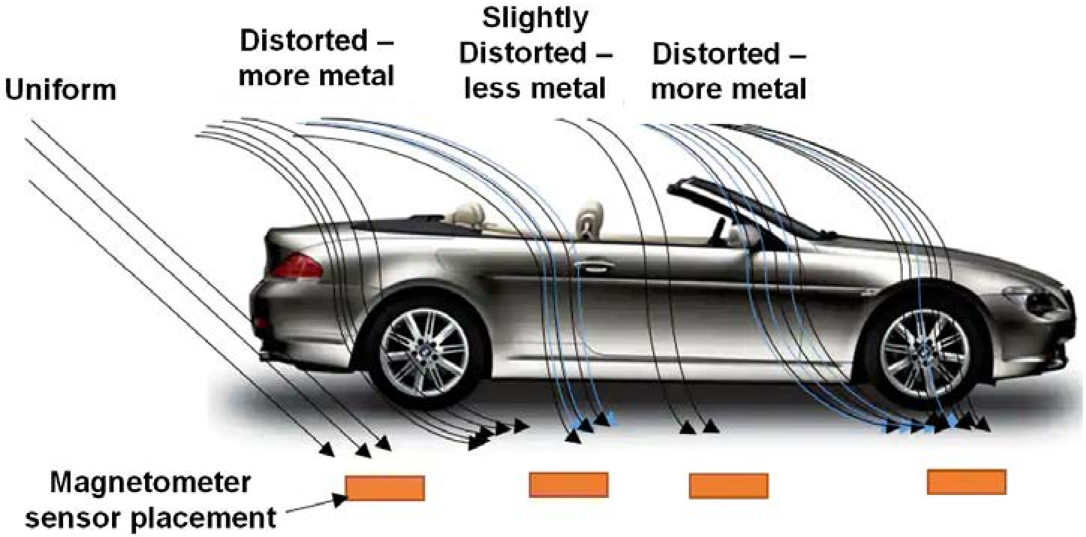

Navigation in GPS Denied Environments
www.hoveringsolutions.com

Tracking of Moving Metallic or Magnetic Object
blog.nxp.com

Magnetometers Comparison

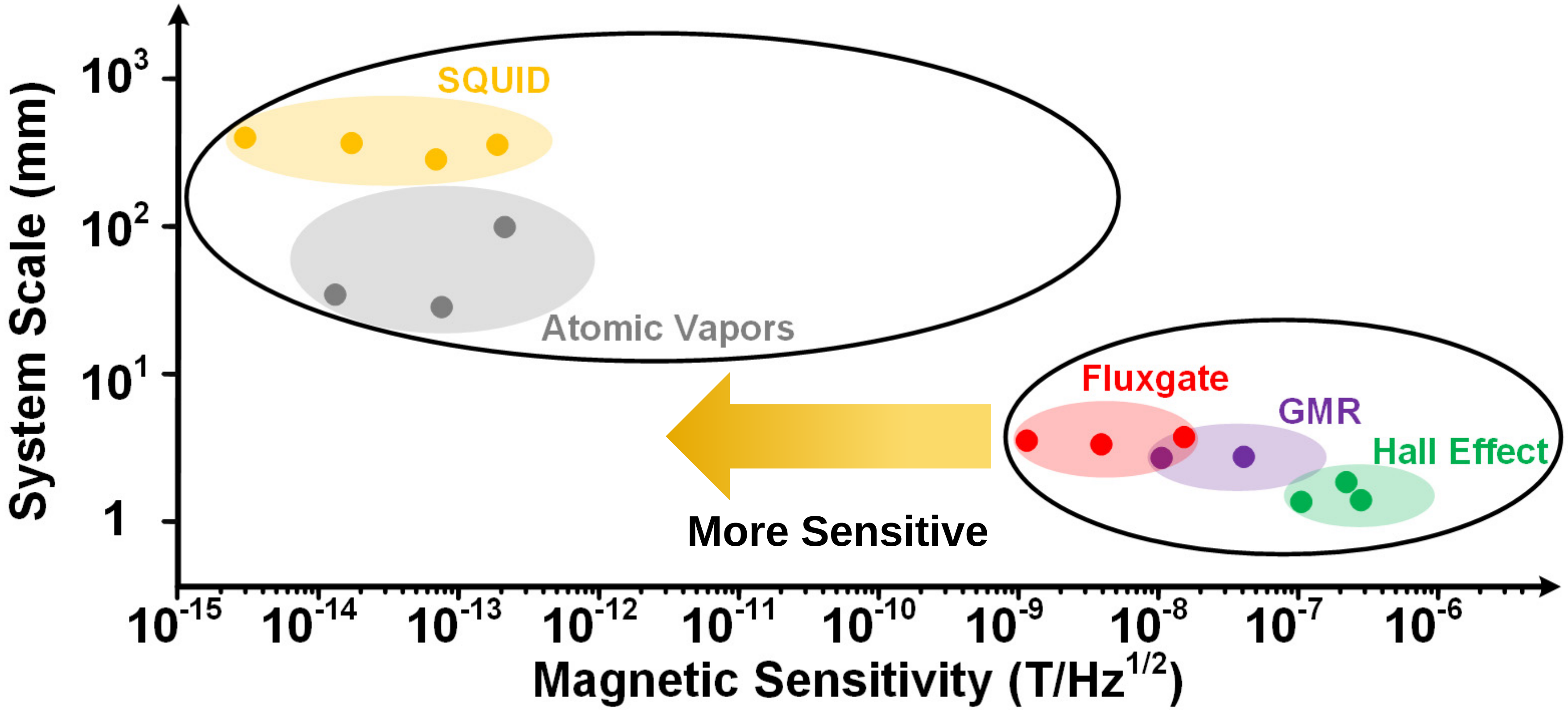

© 2019 IEEE

Magnetometers Comparison

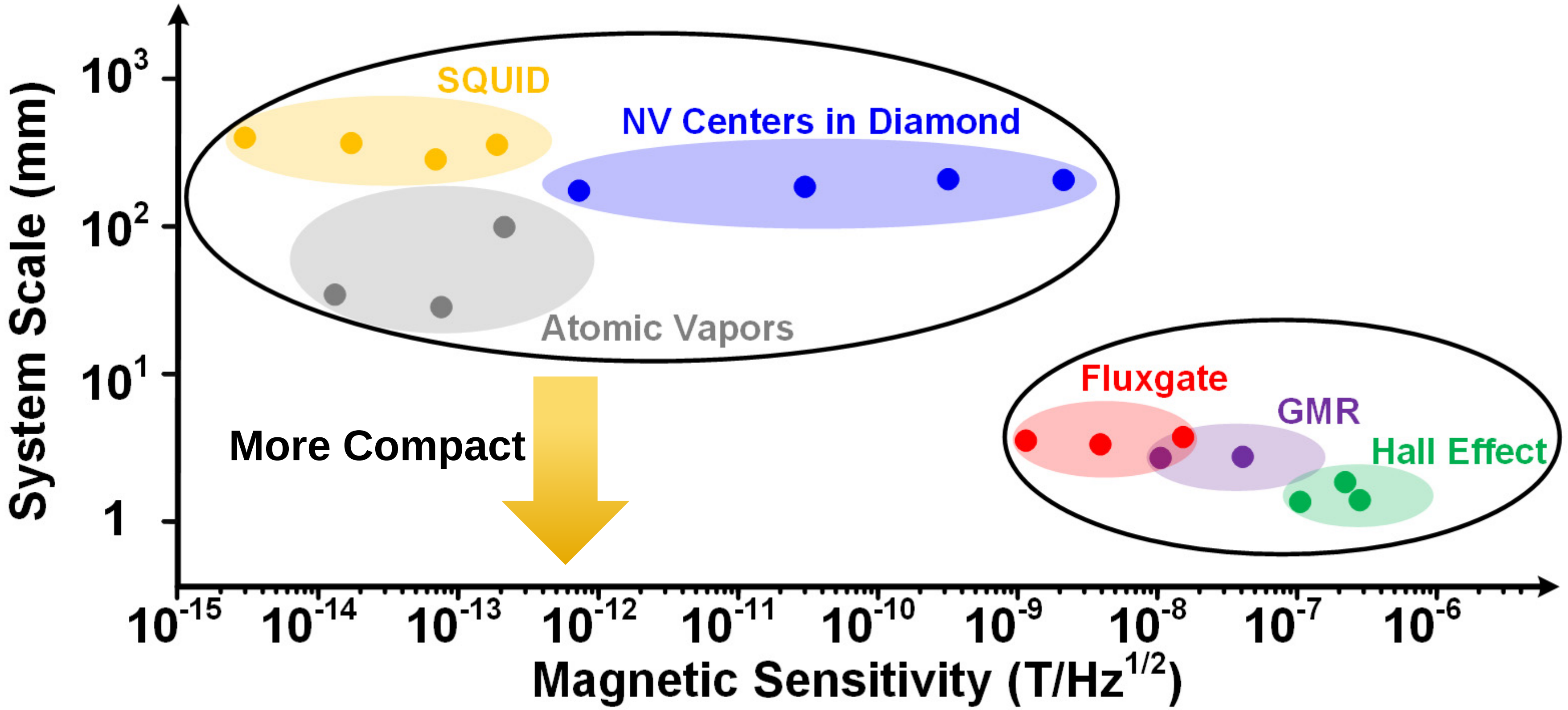

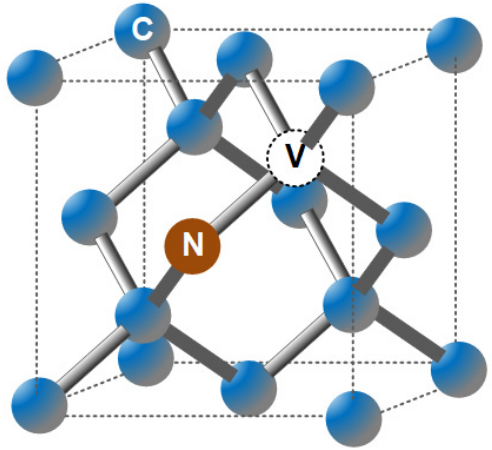

Nitrogen Vacancy (NV) Center in Diamond

- Sub-nT magnetic sensitivity
- Ambient conditions
- Vector field measurements
- Large dynamic range

© 2019 IEEE

NV Centers in Diamond for Quantum Sensing

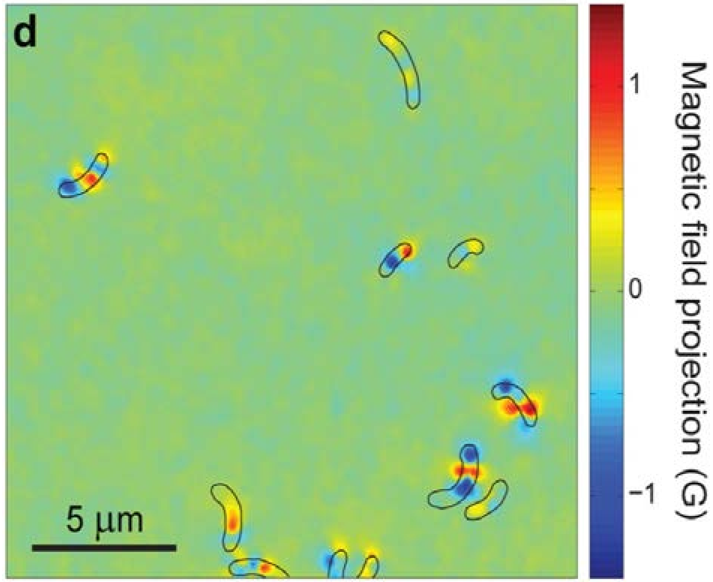

Bacteria Magnetic Imaging
D. Le Sage, et al., Nature 2013

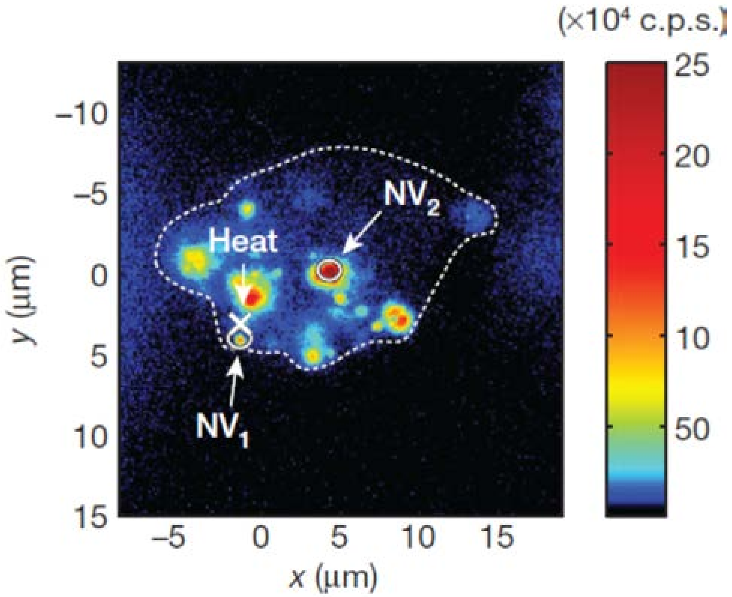

Thermometry in a Living Cell
G. Kucsko, et al., Nature 2013

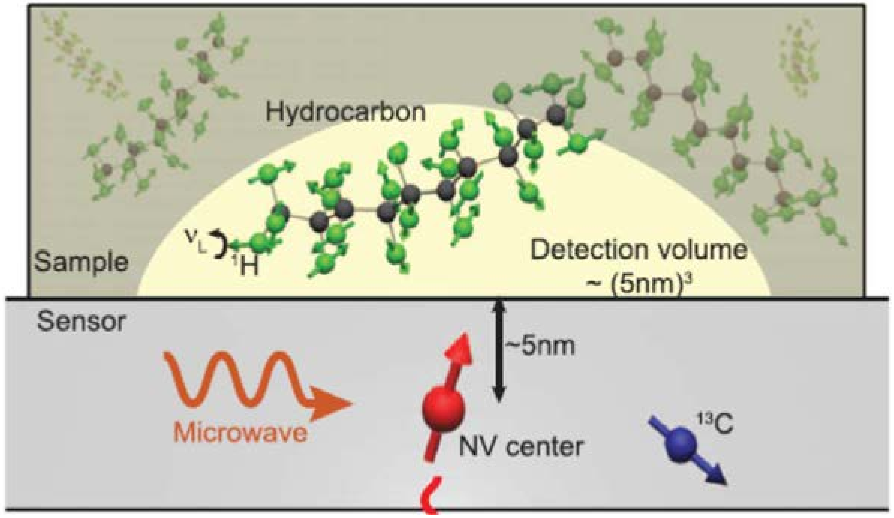

Nuclear Magnetic Resonance Spectroscopy
T. Staudacher, et al., Science 2013

© 2019 IEEE

Hybrid CMOS-Diamond Quantum Systems

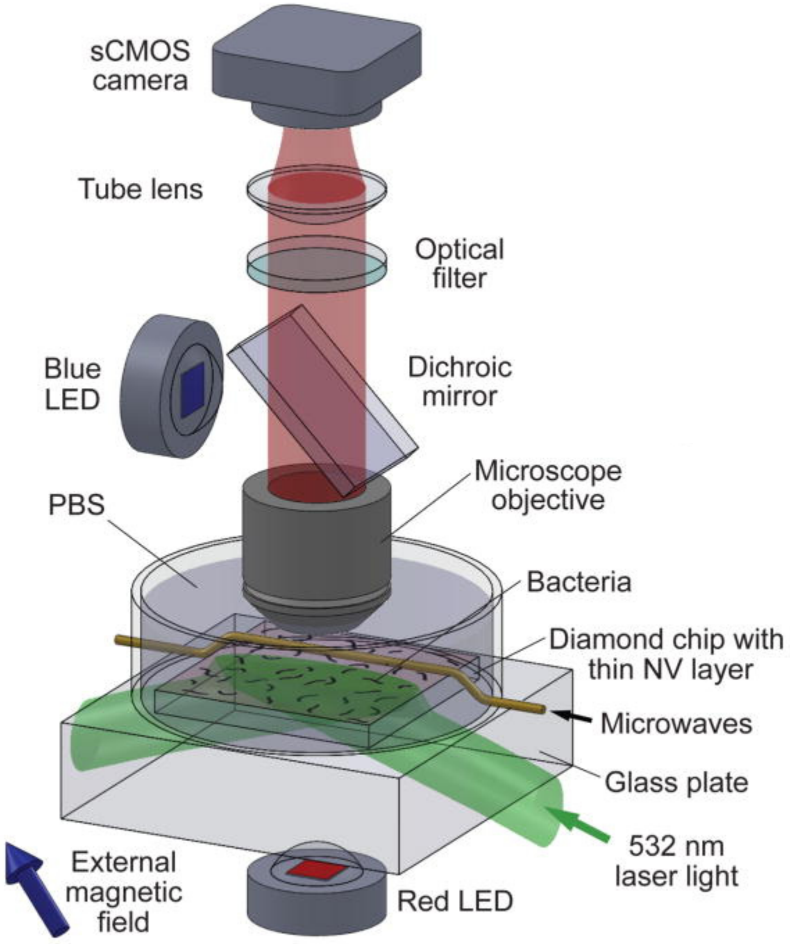

Bacteria Magnetic Imaging
D. Le Sage, et al., Nature 2013

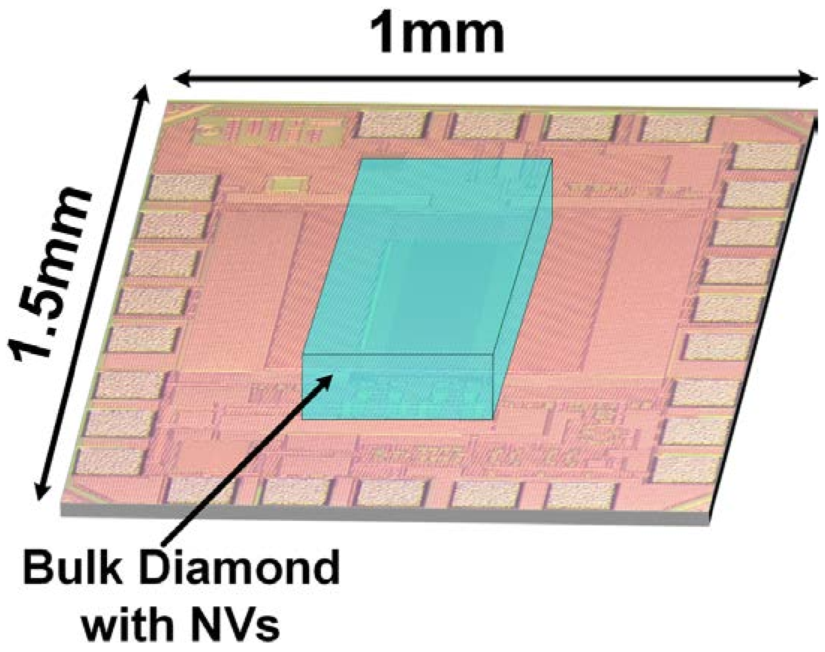

High Precision Sensors

High Resolution Imagers

Scalable Information Processing Systems

Outline

- Introduction
- Magnetometry Principle Using NV Centers in Diamond
- Scalable CMOS-Diamond Hybrid Magnetometer
  – Uniform Microwave Array Design
  – Talbot Effect-Based Optical Filter
  – Complete System Integration
- Measurement Results and Real-Time Demo
- Conclusions

NV Centers in Diamond Magnetometer

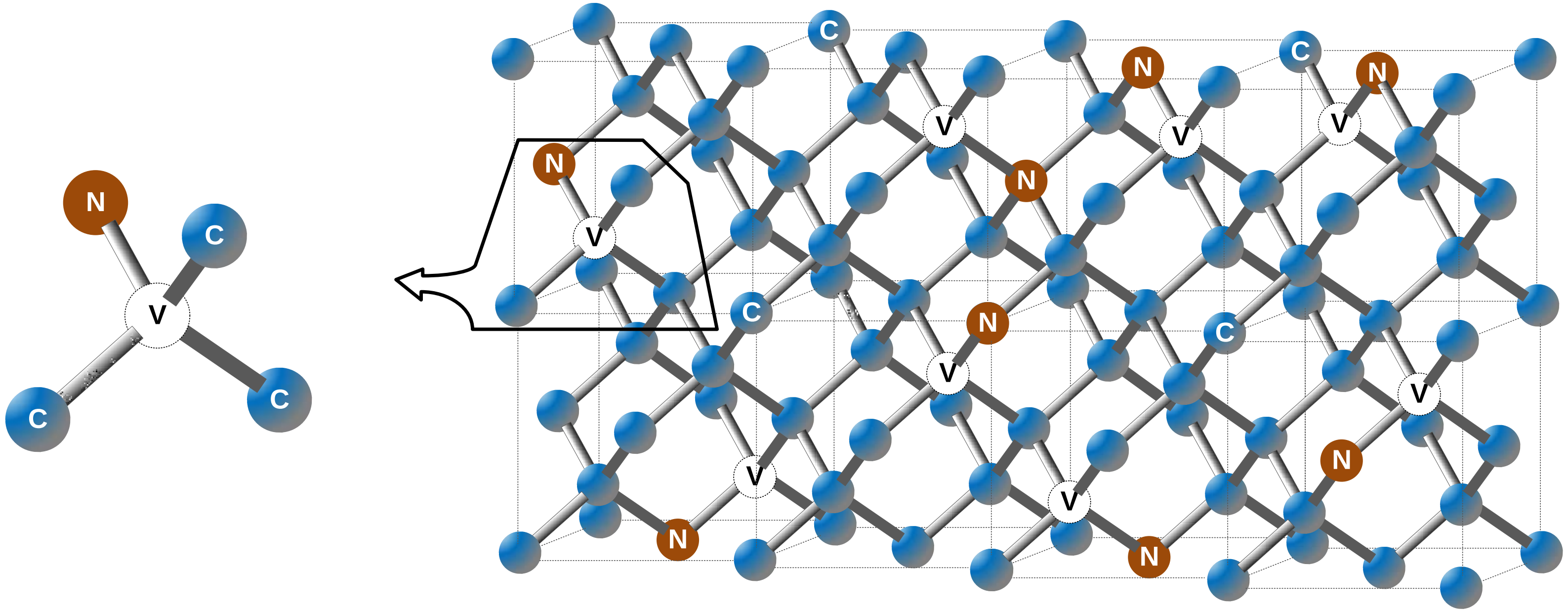

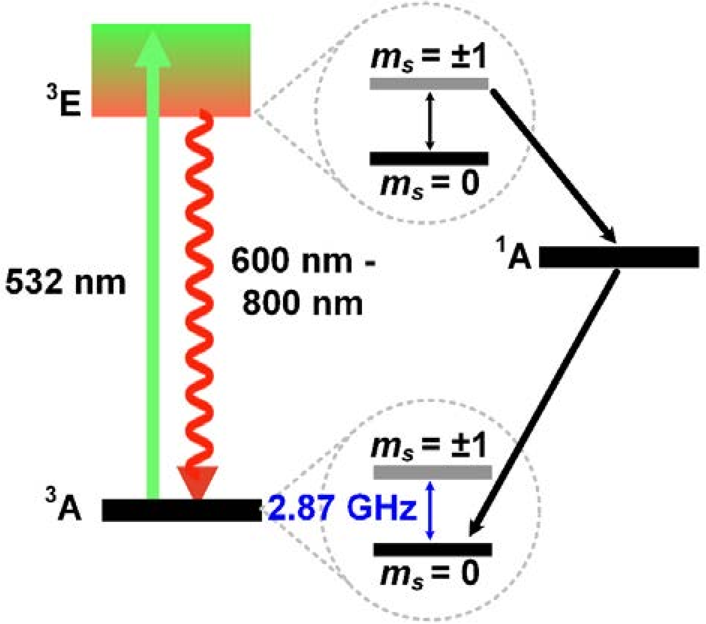

- Optically detected magnetic resonance (ODMR)

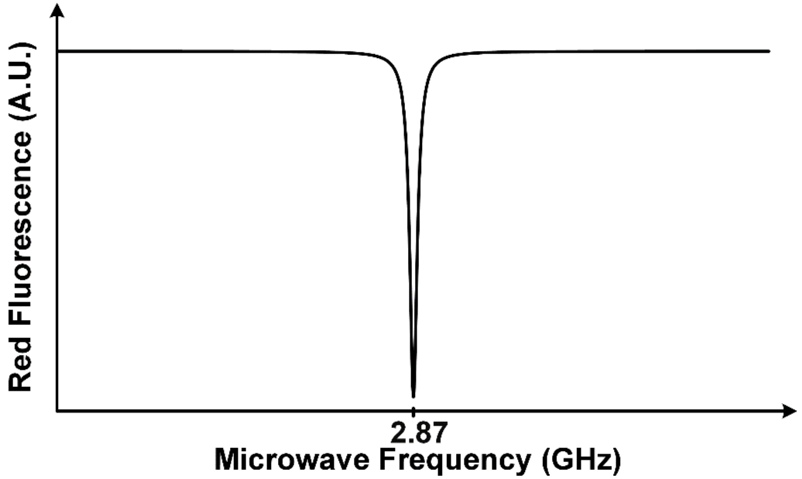

© 2019 IEEE

NV Centers in Diamond Magnetometer

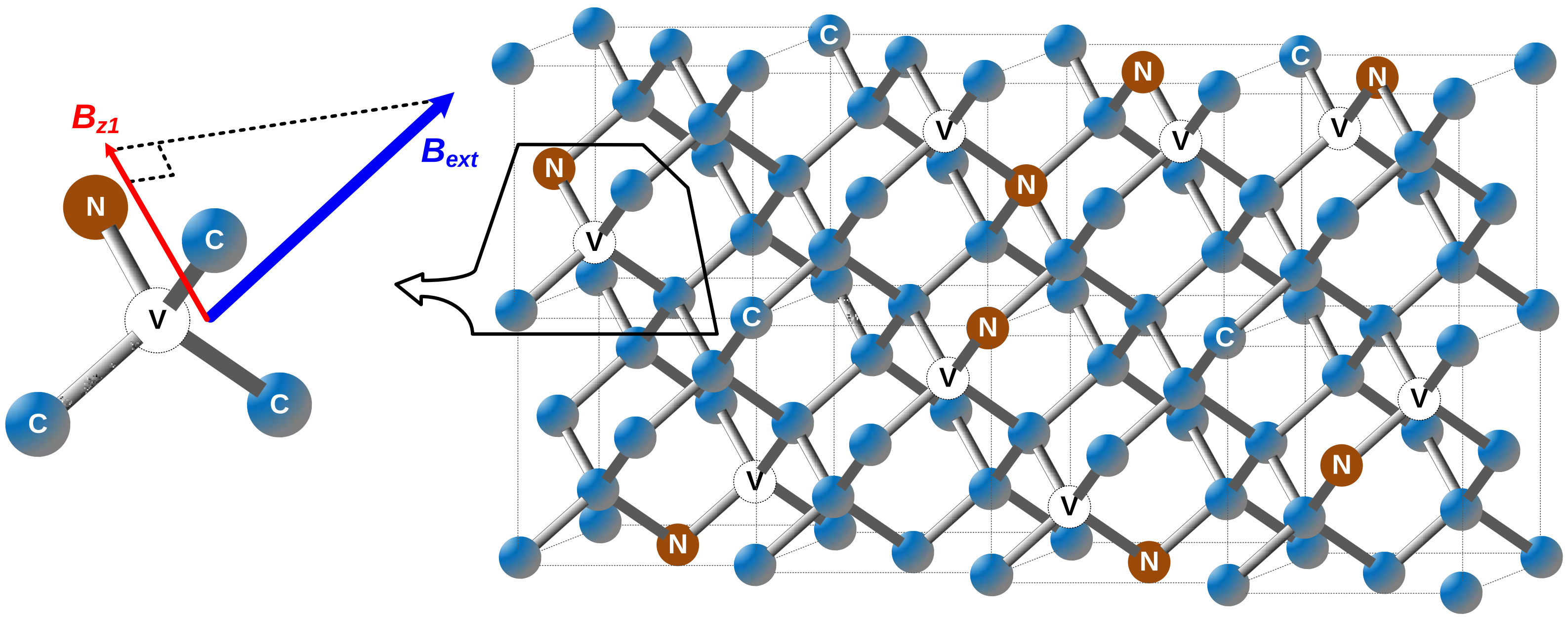

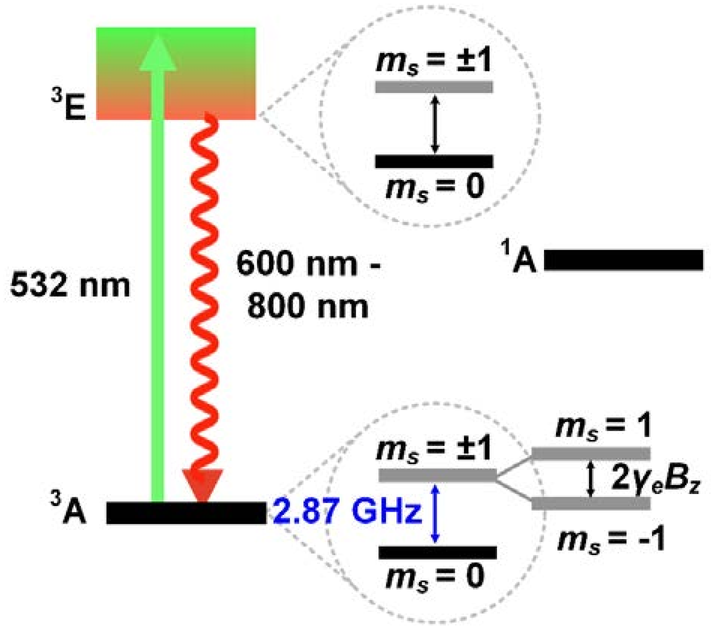

- Optically detected magnetic resonance (ODMR)
- External magnetic field is measured using Zeeman splitting (γ_e = 28GHz/T)

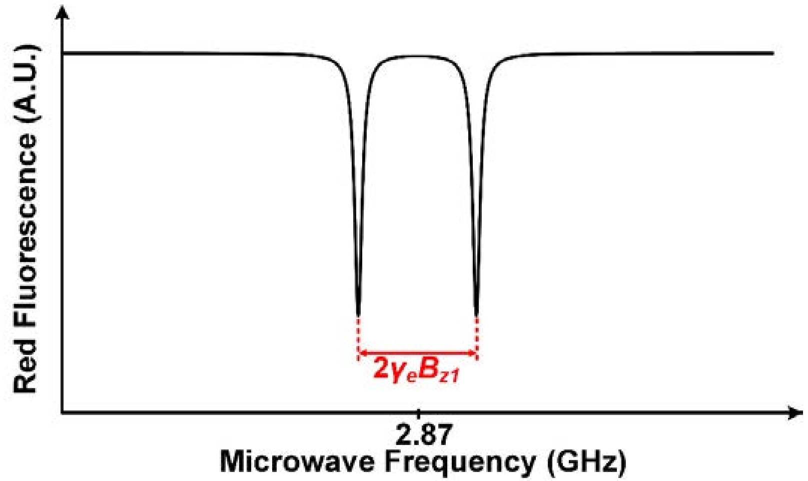

© 2019 IEEE

NV Centers in Diamond Magnetometer

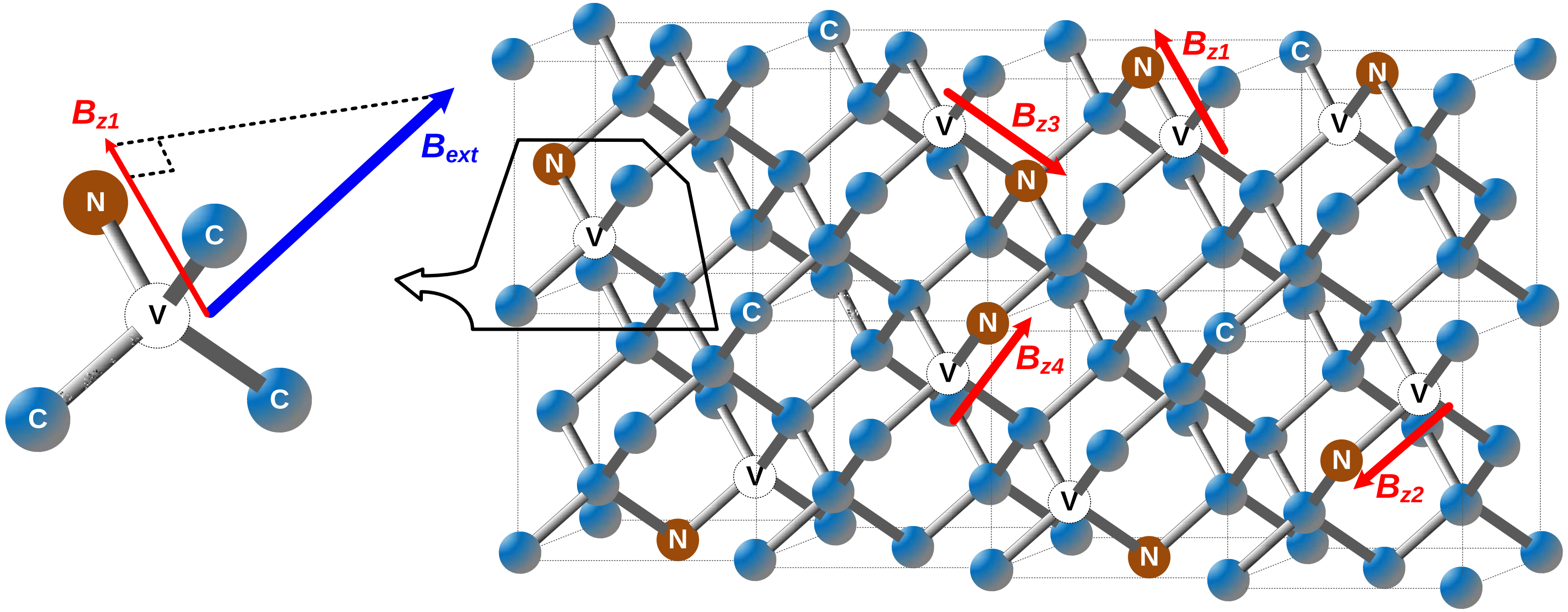

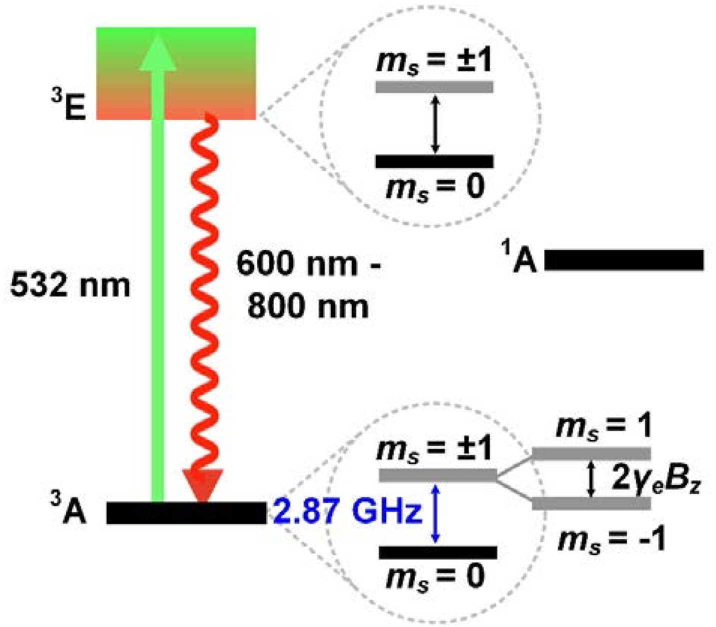

- **Optically detected magnetic resonance (ODMR)**
- **External magnetic field is measured using Zeeman splitting (γ_e = 28GHz/T)**
- **B_{z1}, B_{z2}, B_{z3}, B_{z4} are the projections of B_{ext} along the NV axes**

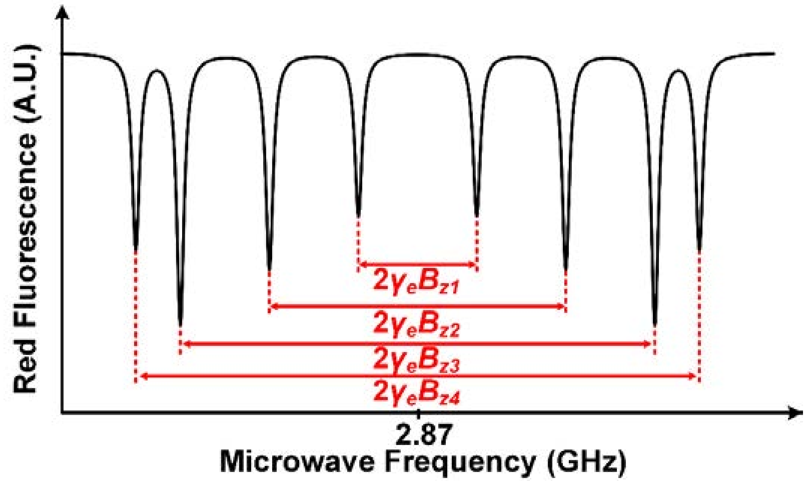

© 2019 IEEE
International Solid-State Circuits Conference

Integrated CMOS-Diamond Quantum Magnetometer

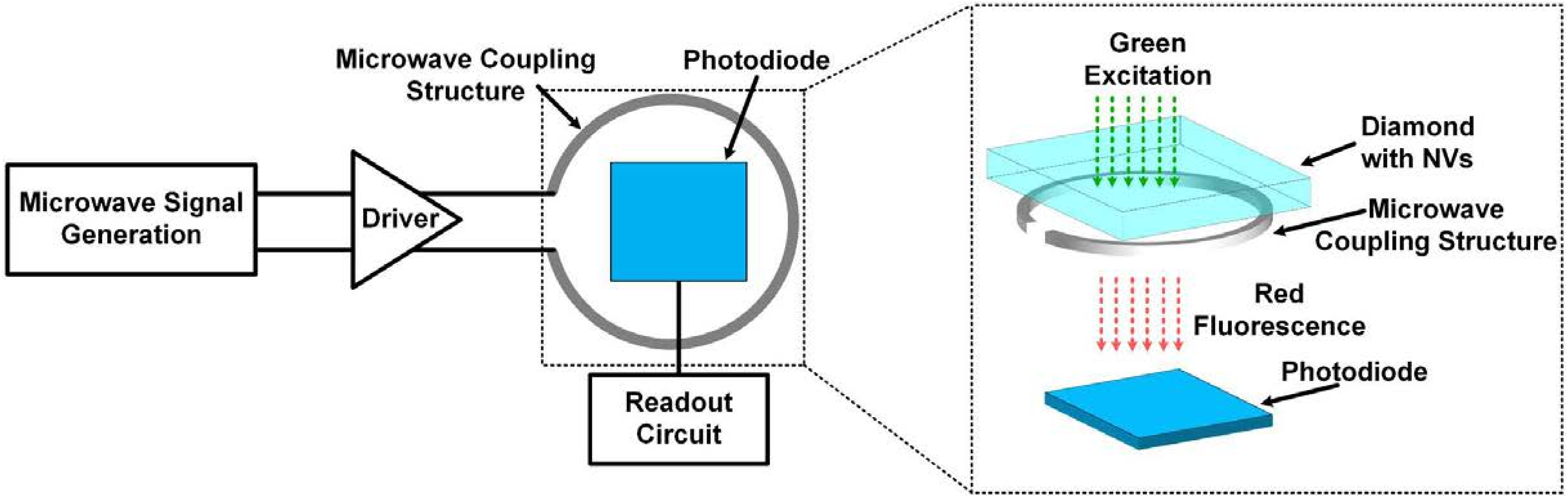

- ~2.87GHz strong homogenous microwave field for spin manipulation
  - Increases the contrast
  - Drives the NVs with equal strength to decrease linewidth broadening
- Photo-detection for red fluorescence (I_{Red})
  - Increases with the number of NV centers

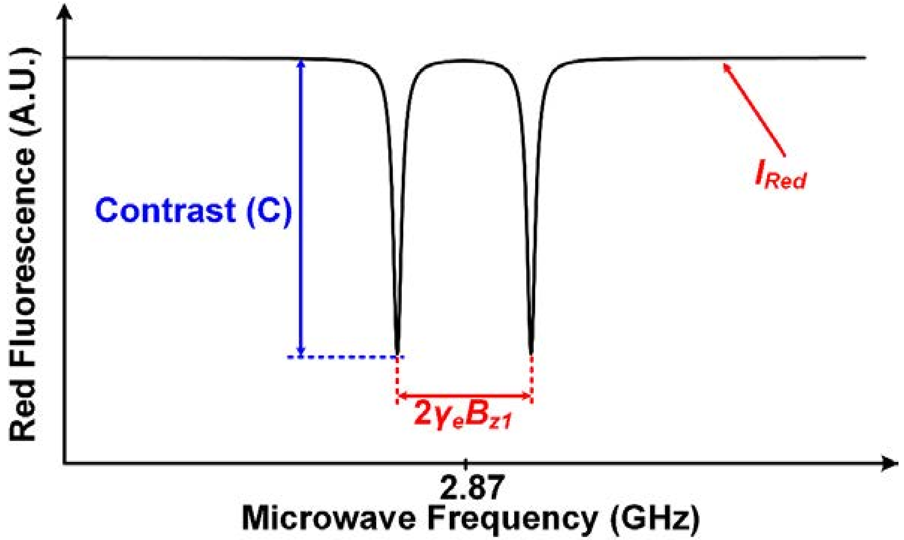

© 2019 IEEE

Integrated CMOS-Diamond Quantum Magnetometer

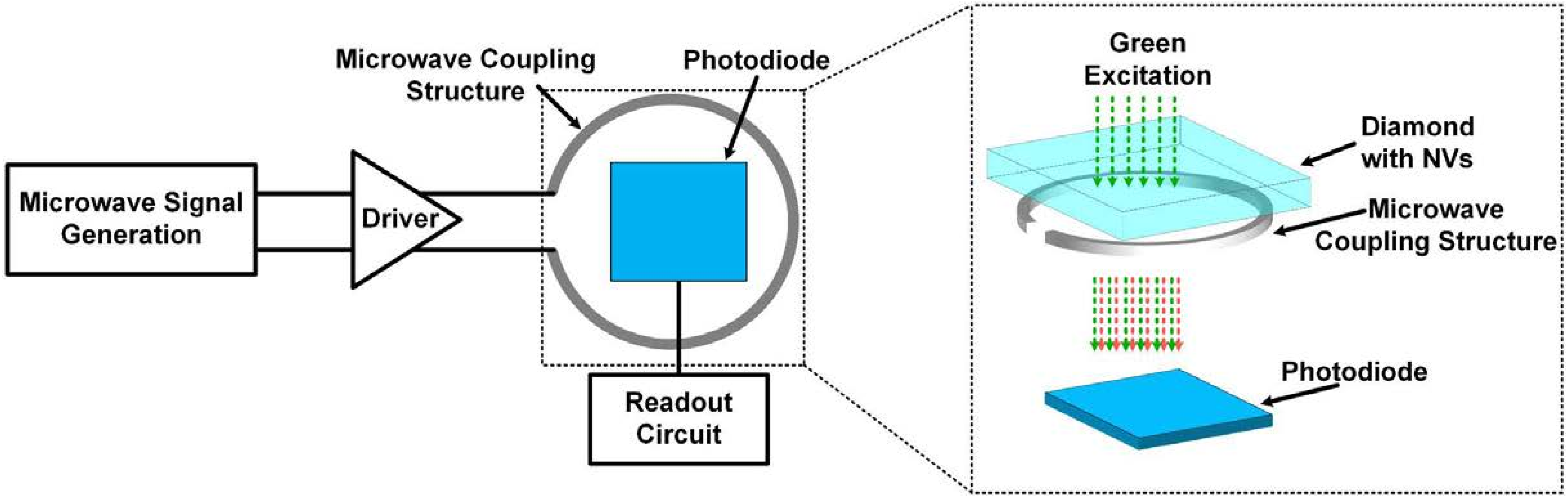

- **Green light is not absorbed completely by the diamond**
  - **Decreases the contrast**
  - **Increases the shot noise**

$$I_n^2 = 2q(I_{Red} + I_{Green})^2 \Delta f$$

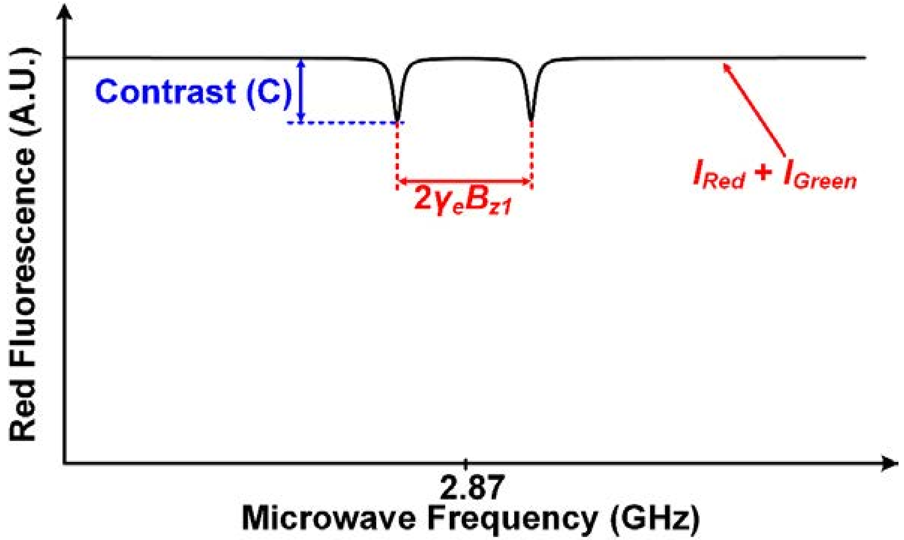

Integrated CMOS-Diamond Quantum Magnetometer

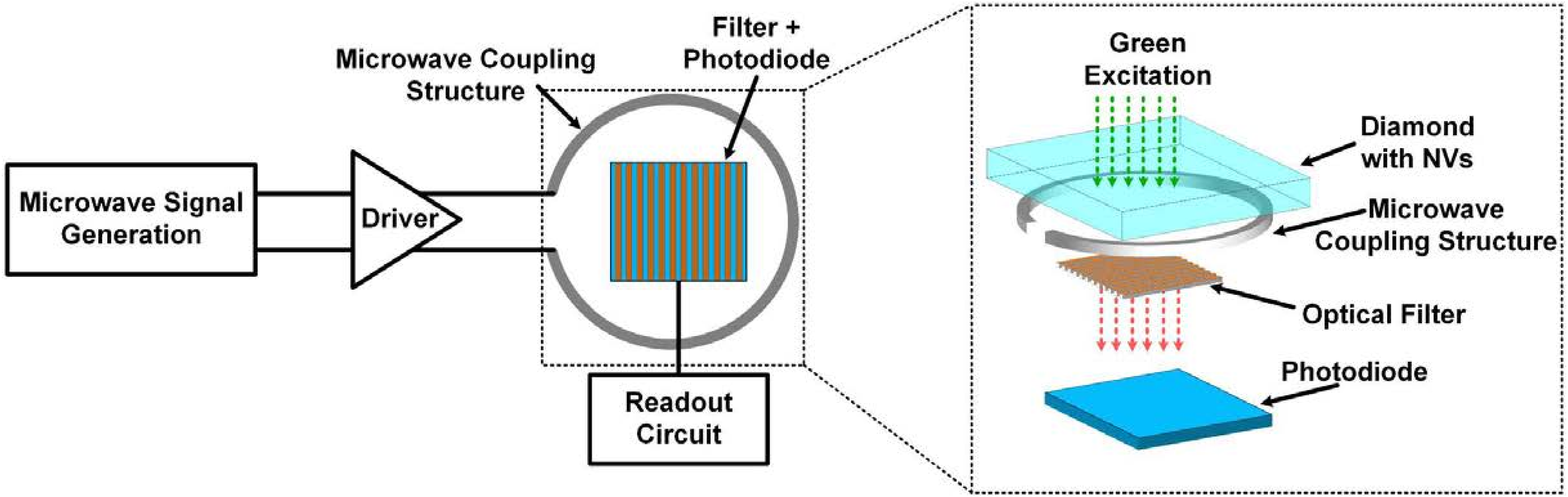

- Green light is not absorbed completely by the diamond
  - Decreases the contrast
  - Increases the shot noise

$$I_n^2 = 2q(I_{Red} + I_{Green})^2 \Delta f$$

- Optical filtering for green light is needed

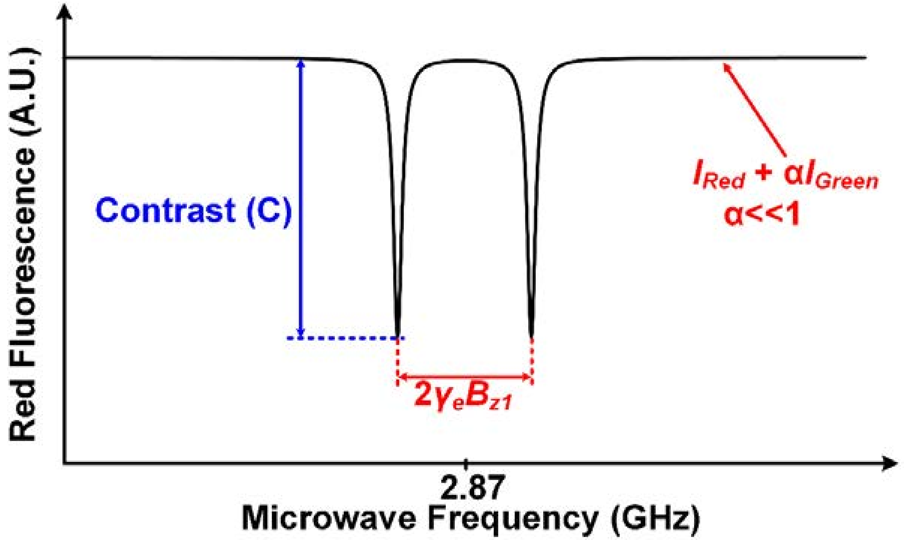

© 2019 IEEE

CMOS-Diamond Magnetometer Design Constraints

- **The sensitivity (η) is the minimum detectable magnetic field (T/$\sqrt{Hz}$)**
- **$\eta \propto$ 1/SNR**

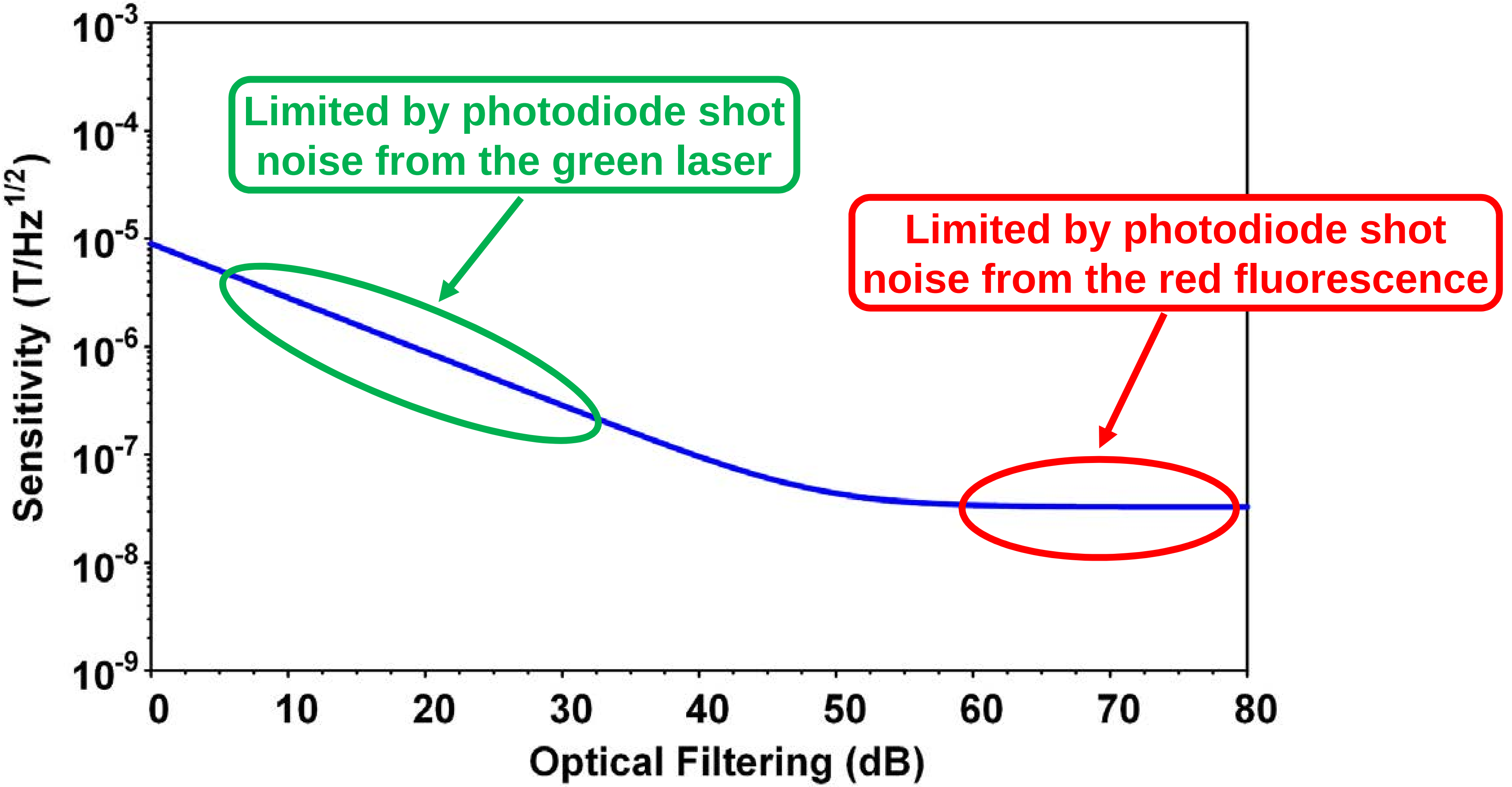

© 2019 IEEE

CMOS-Diamond Magnetometer Design Constraints

- **The sensitivity (η) is the minimum detectable magnetic field (T/$\sqrt{\text{Hz}}$)**
- **$\eta \propto$ 1/SNR**

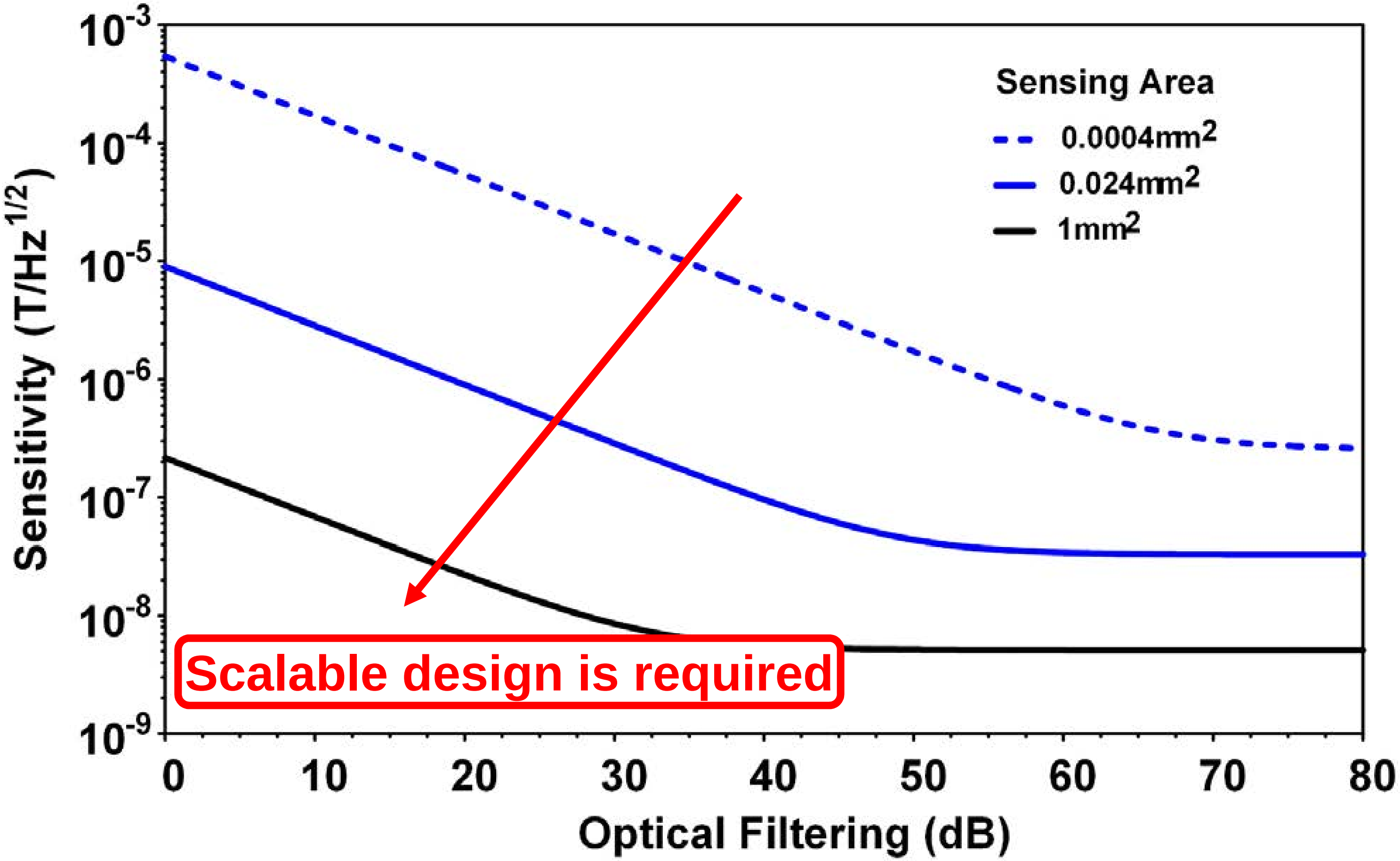

© 2019 IEEE

Outline

- Introduction
- Magnetometry Principle Using NV Centers in Diamond
- **Scalable CMOS-Diamond Hybrid Magnetometer**
  - Uniform Microwave Array Design
  - Talbot Effect-Based Optical Filter
  - Complete System Integration
- Measurement Results and Real-Time Demo
- Conclusions

Microwave Coupling Structure

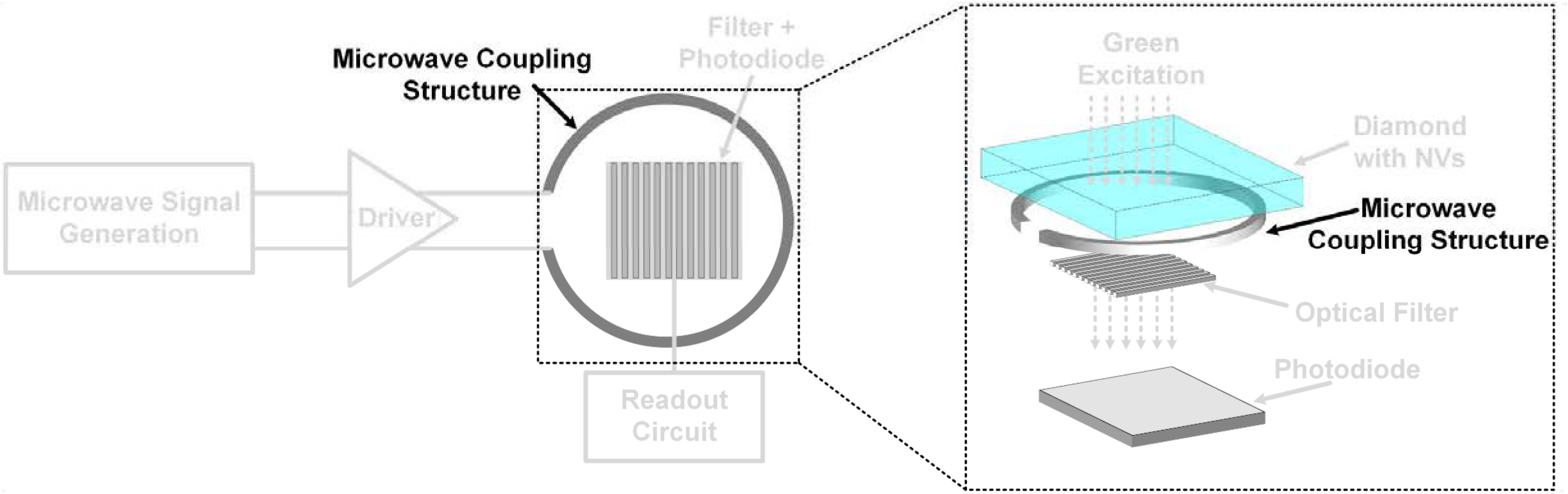

- A scalable structure with homogeneous field profile generation is required
- Previously straight wires and loops are commonly used
  - Microwave field homogeneity is achieved within only a small area
  - Scaling up for larger areas is hard

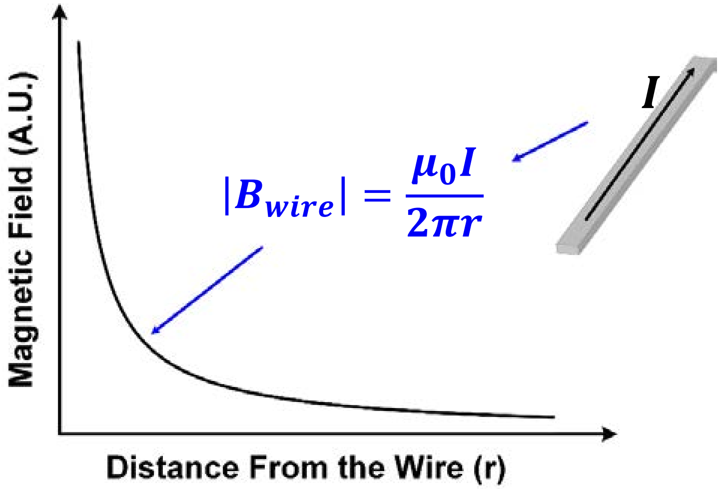

© 2019 IEEE

Uniform Sheet of Current

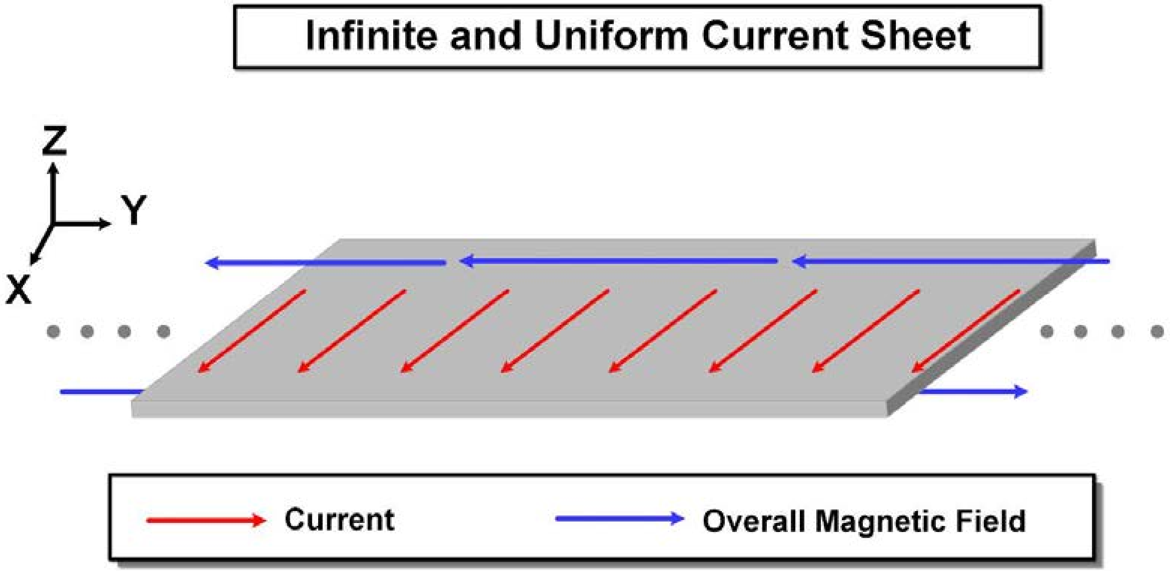

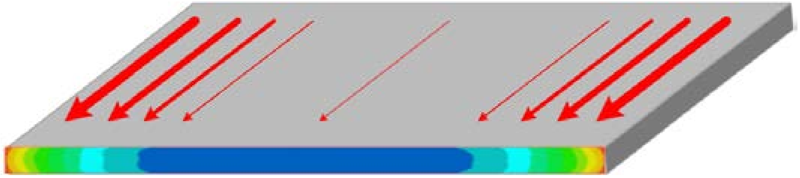

RF Current Redistribution in a Single Flat Conductor

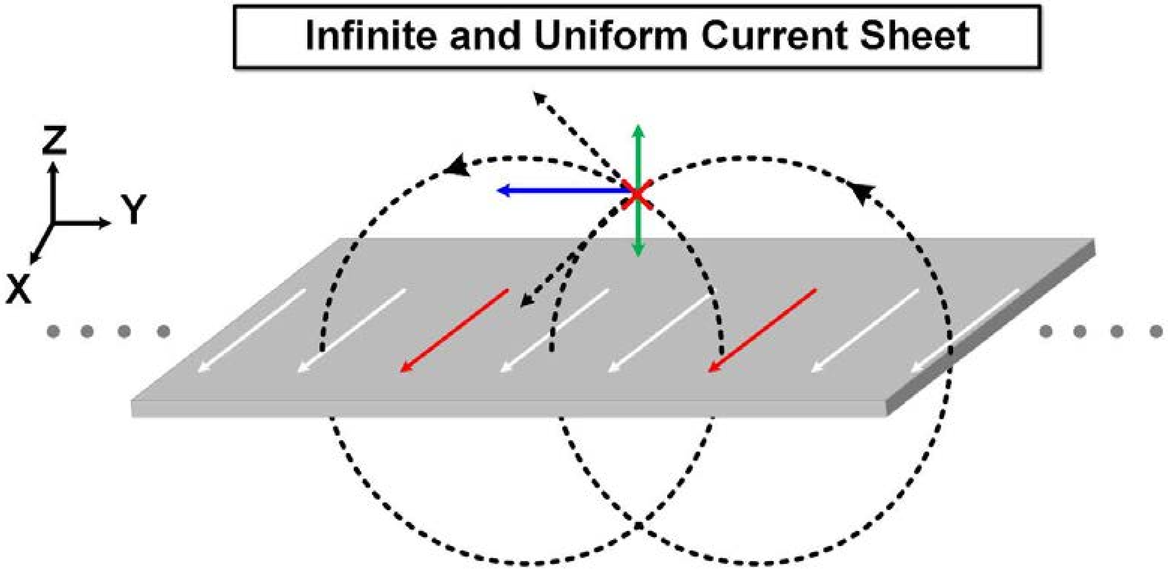

- **The total magnetic field component at y direction from the sheet is:**

$$\boldsymbol{B_y = \frac{\mu_0 J_s}{2}}$$

where J_s is the current density across the sheet

Uniform Sheet of Current

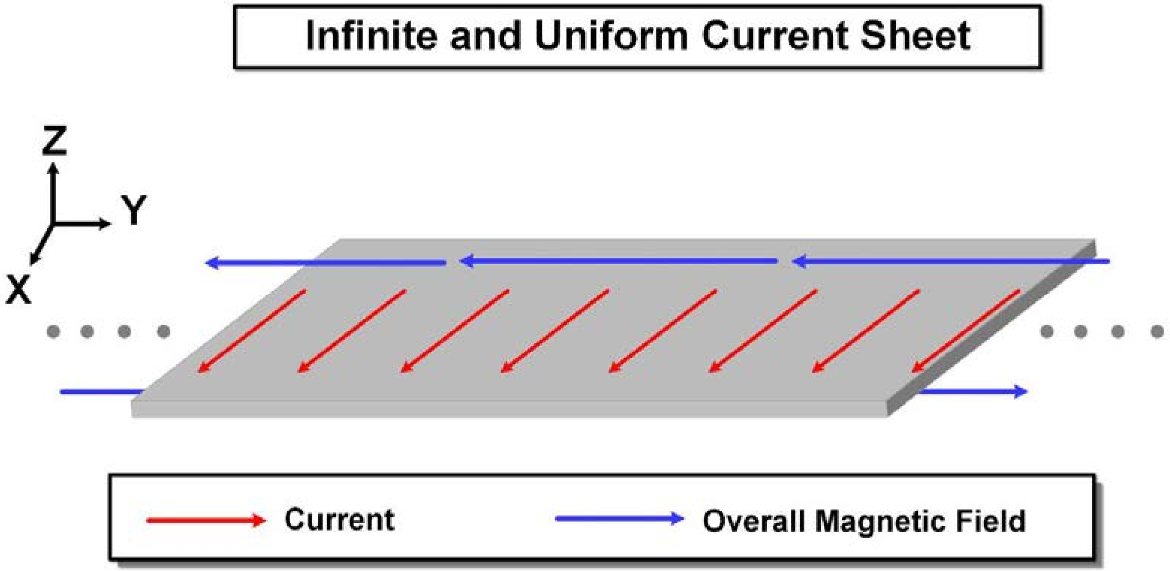

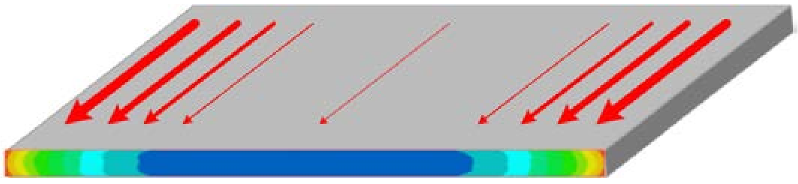

RF Current Redistribution in a Single Flat Conductor

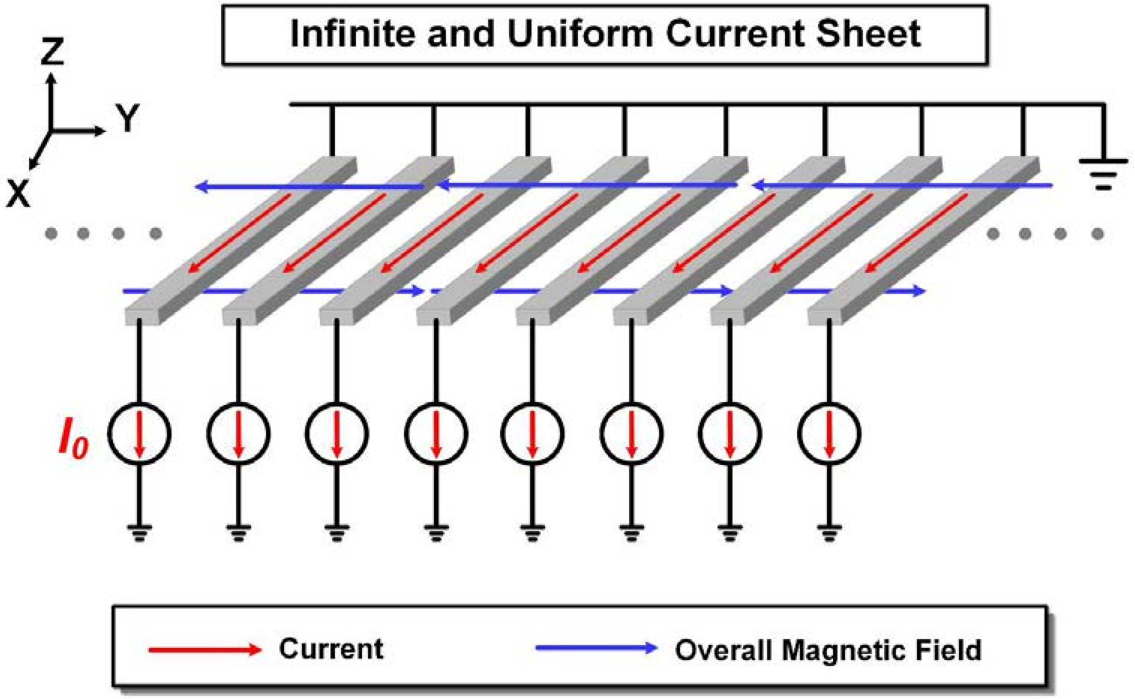

- Regulation and arbitrary control of local currents using transistors
- Highly-scalable, CMOS-enabled structure
  - This design can be extended to larger areas

Scalable Microwave Array

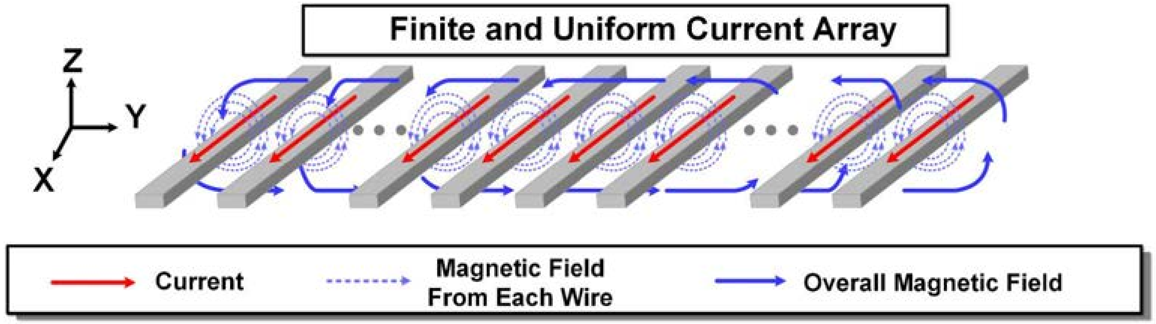

- The magnetic field at location (*0,y,z*) of each conductor located at (*0,y_n,0*) is:

$$|B_n| = \frac{\mu_0 I_n}{2\pi r} = \frac{\mu_0 I_n}{2\pi\sqrt{(y-y_n)^2+z^2}} \;;\, y_n = nd$$

where d is the array pitch size

- The total magnetic field component at y direction from all the conductors is:

$$B_y = \sum_{-\frac{N}{2}}^{\frac{N}{2}} B_{y_n} = \sum_{-\frac{N}{2}}^{\frac{N}{2}} \frac{\mu_0 I_n}{2\pi} \frac{z}{(y-y_n)^2+z^2}$$

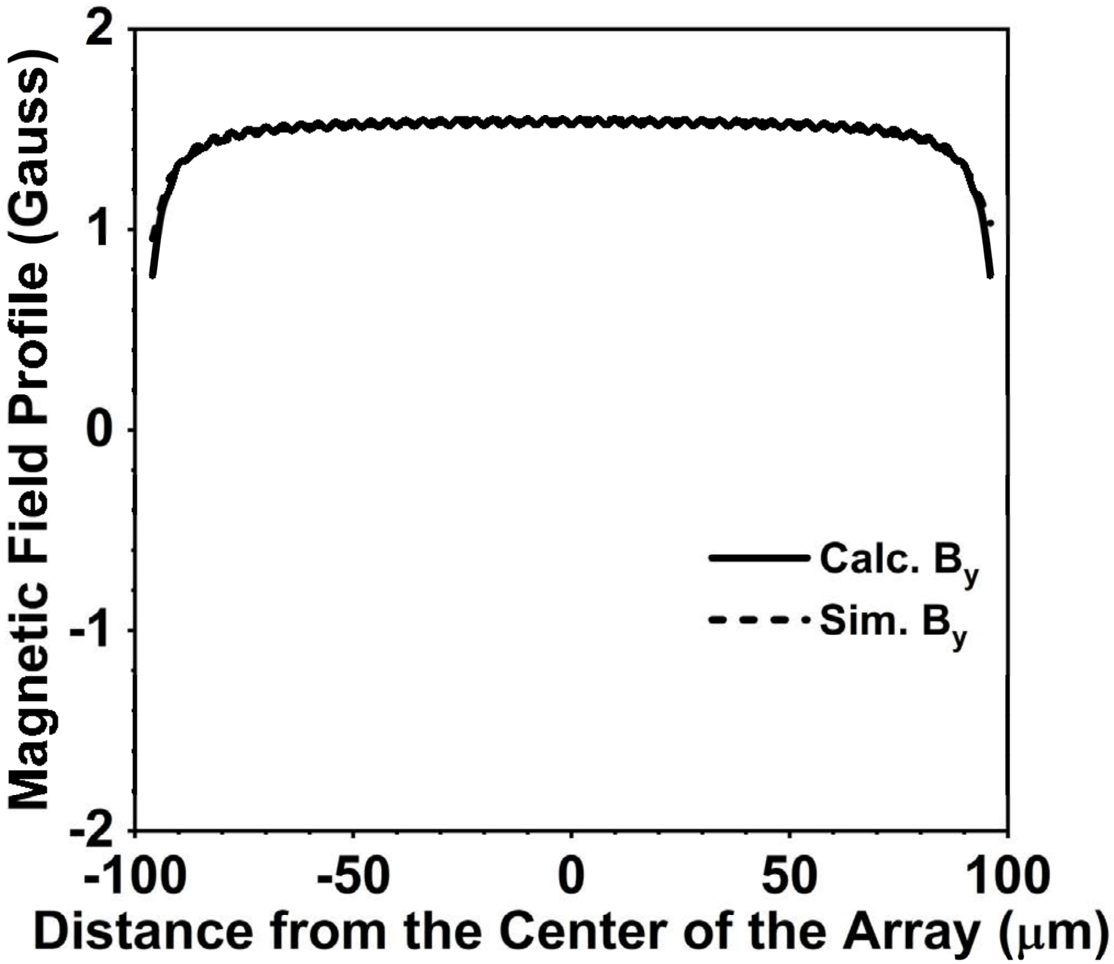

© 2019 IEEE

Scalable Microwave Array

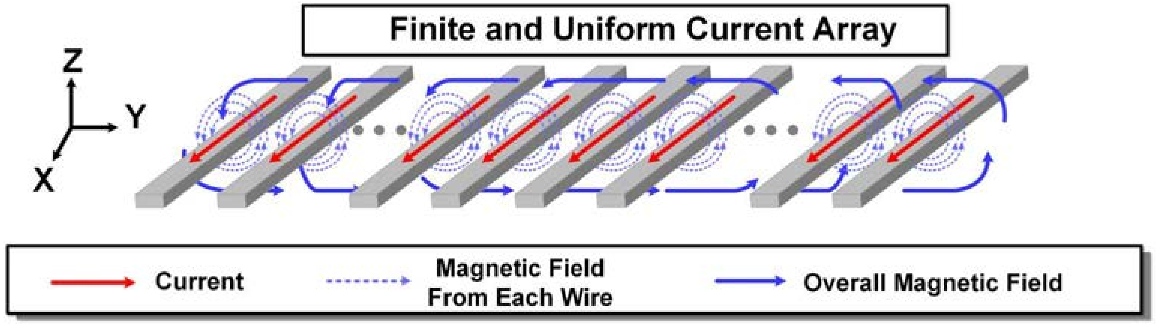

- The total magnetic field component in z direction from all the conductors is:

$$B_z = \sum_{-\frac{N}{2}}^{\frac{N}{2}} B_{z_n} = \sum_{-\frac{N}{2}}^{\frac{N}{2}} \frac{\mu_0 I_n}{2\pi} \frac{y - y_n}{(y - y_n)^2 + z^2}$$

$$\approx \frac{\mu_0 I_n}{4\pi} \left(\ln\left[\left(y - \frac{N}{2} d \right)^2 + z^2 \right] - \ln\left[\left(y + \frac{N}{2} d \right)^2 + z^2 \right] \right)$$

where $y_n = nd$ and d is the array pitch size

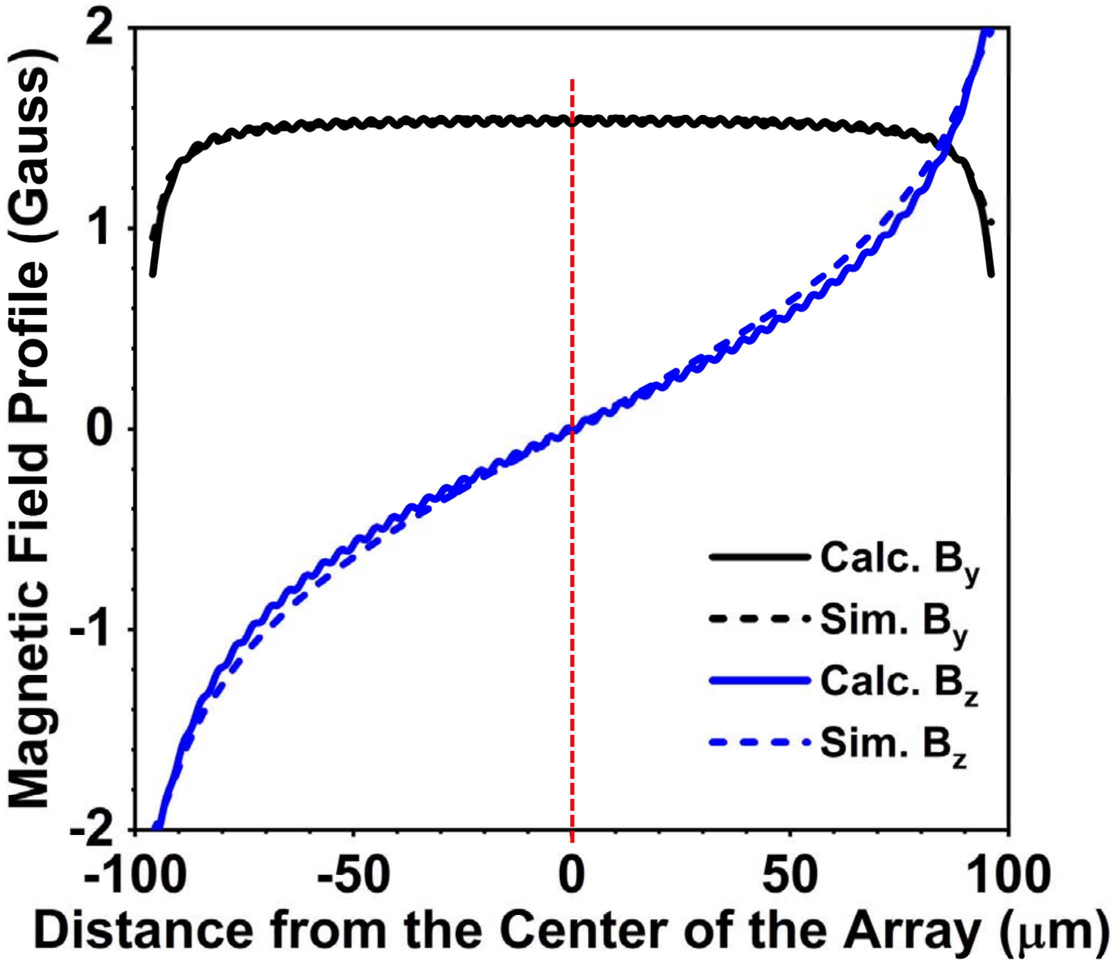

Scalable Microwave Array

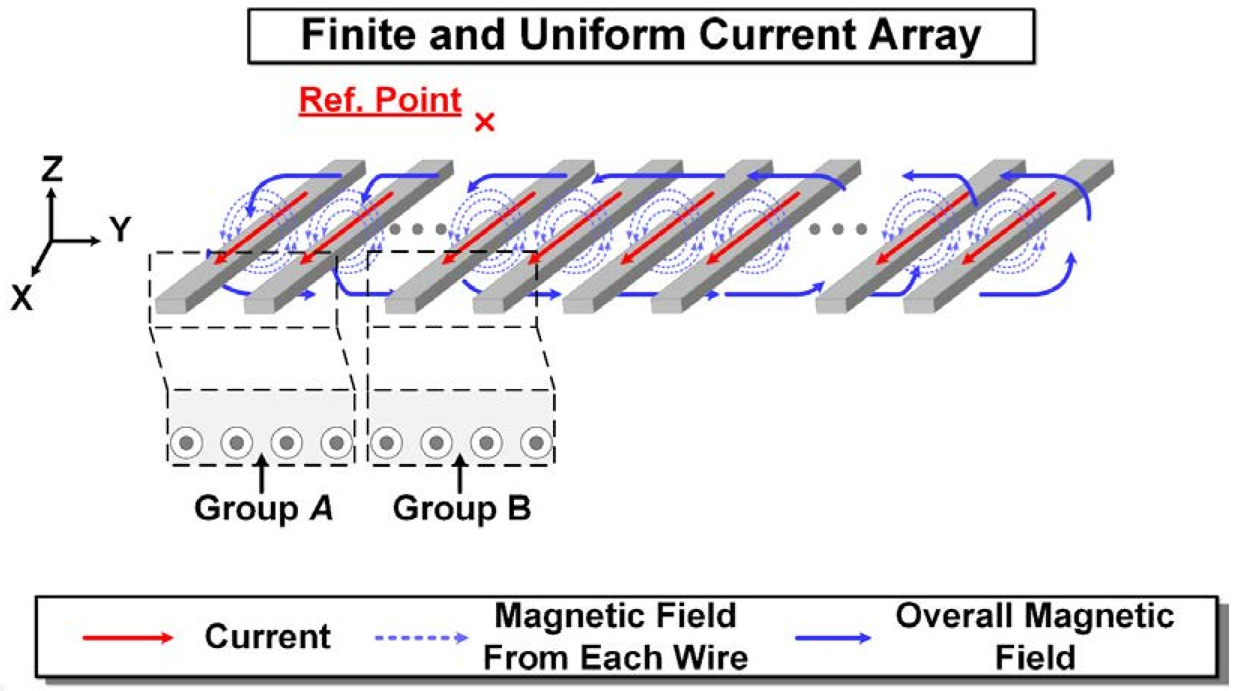

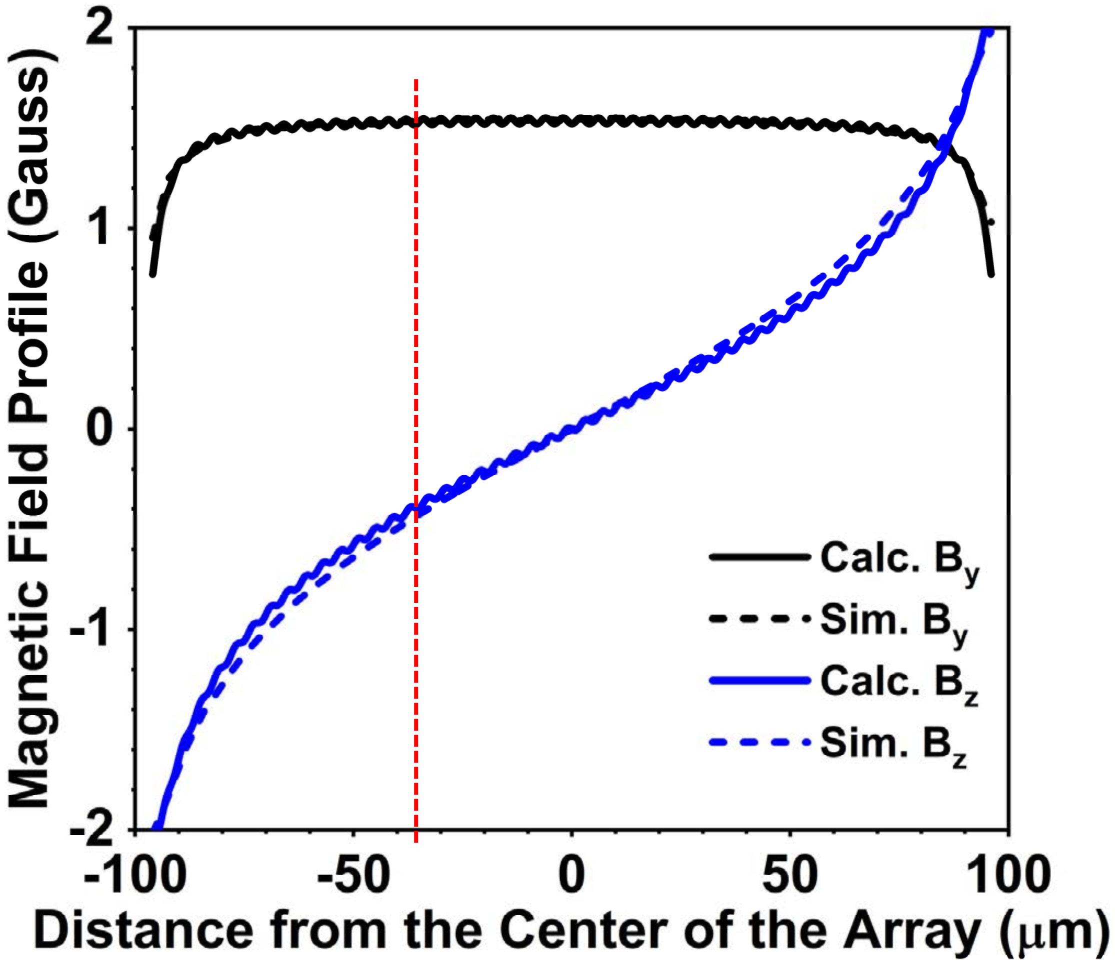

Scalable Microwave Array

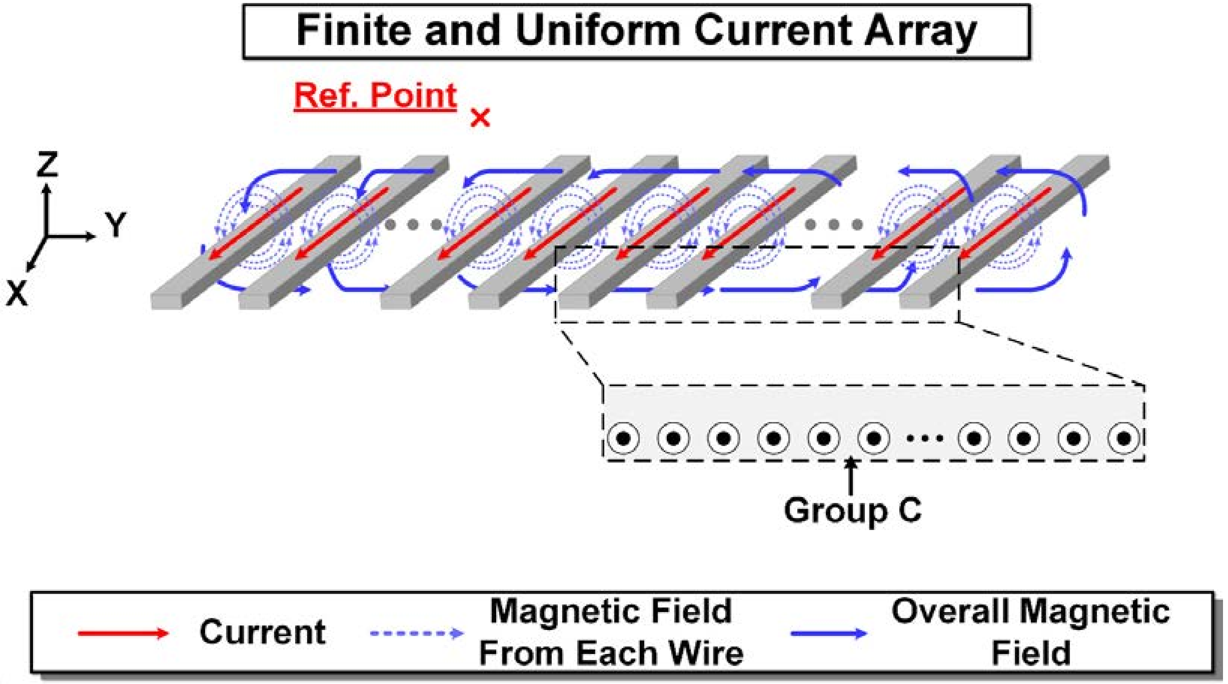

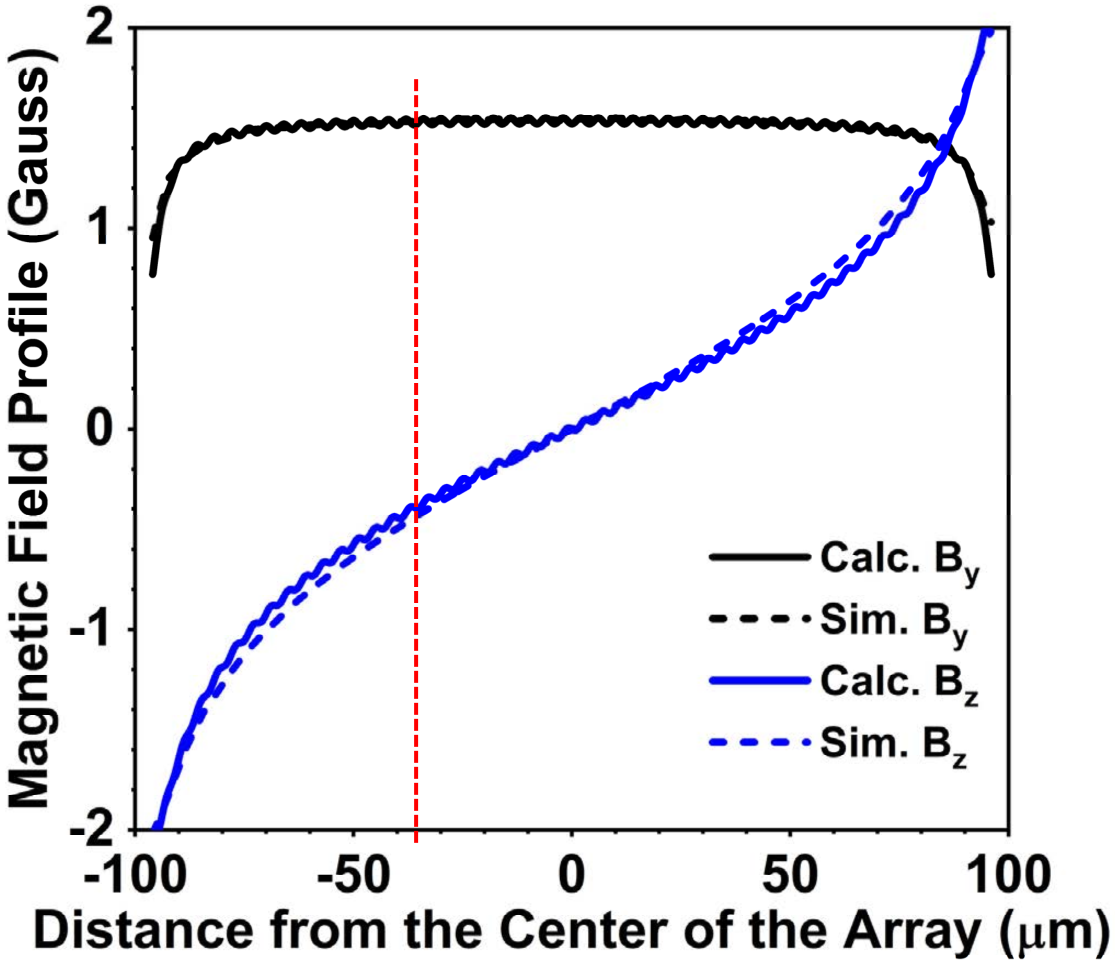

Microwave Array with Uniform Magnetic Field

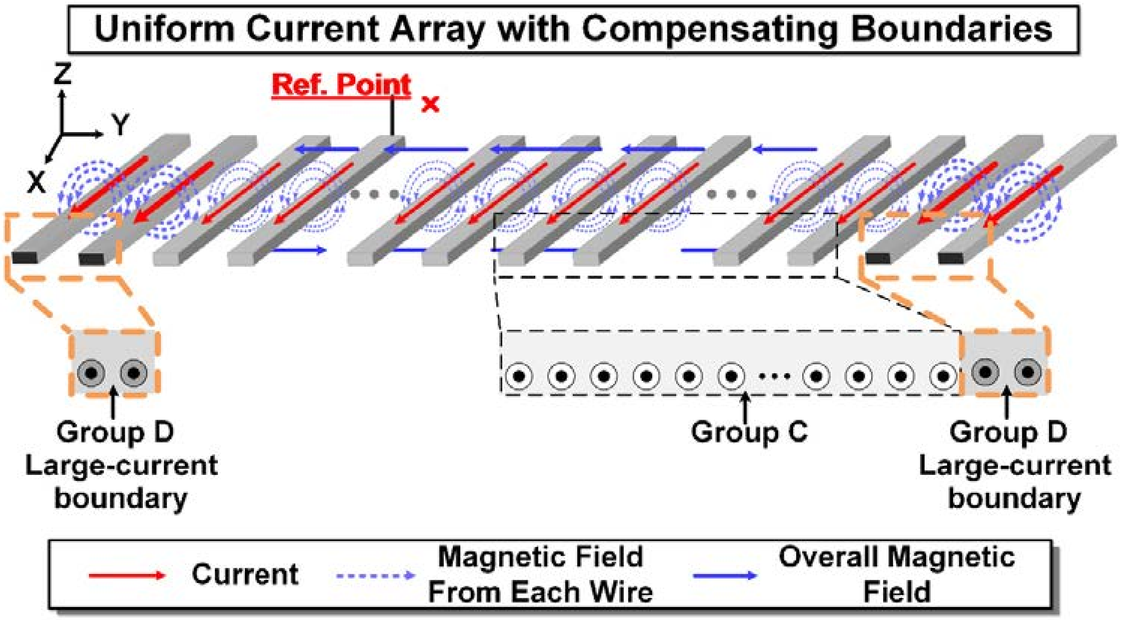

- The total magnetic field component in z direction from all the conductors is:

$$B_z = \sum_{-\frac{N}{2}-l}^{-\frac{N}{2}-1} \beta Q_n + \sum_{-\frac{N}{2}}^{\frac{N}{2}} Q_n + \sum_{\frac{N}{2}+1}^{\frac{N}{2}+l} \beta Q_n$$

$$\approx \frac{\mu_0 I_n}{4\pi}\left[(1-\beta)\left(\ln\left[\left(y-\frac{N}{2}d\right)^2+z^2\right]-\ln\left[\left(y+\frac{N}{2}d\right)^2+z^2\right]\right)\right.$$
$$\left.+\beta\left(\ln\left[\left(y-\left(\frac{N}{2}+l\right)d\right)^2+z^2\right]-\ln\left[\left(y+\left(\frac{N}{2}+l\right)d\right)^2+z^2\right]\right)\right]$$

  – $Q_n = \frac{y-y_n}{(y-y_n)^2+z^2}$
  – $y_n = nd$ and d is the array pitch size
  – l is the number of boundary conductors
  – β is the ratio between the boundary and the core conductors currents

Microwave Array with Uniform Magnetic Field

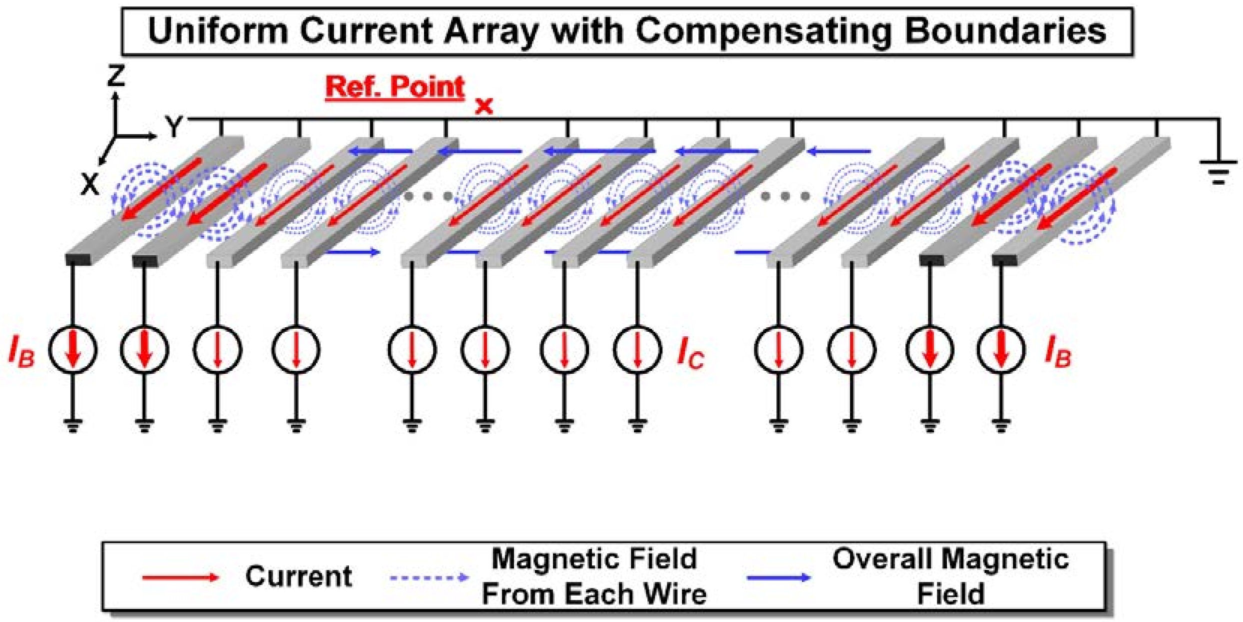

Large boundary current to compensate for the vertical field

- The total magnetic field component in z direction from all the conductors is:

$$B_z = \sum_{-\frac{N}{2}-l}^{-\frac{N}{2}-1} \beta Q_n + \sum_{-\frac{N}{2}}^{\frac{N}{2}} Q_n + \sum_{\frac{N}{2}+1}^{\frac{N}{2}+l} \beta Q_n$$

$$\approx \frac{\mu_0 I_n}{4\pi}\left[(1-\beta)\left(\ln\left[\left(y-\frac{N}{2}d\right)^2+z^2\right]-\ln\left[\left(y+\frac{N}{2}d\right)^2+z^2\right]\right)\right.$$
$$\left.+\beta\left(\ln\left[\left(y-\left(\frac{N}{2}+l\right)d\right)^2+z^2\right]-\ln\left[\left(y+\left(\frac{N}{2}+l\right)d\right)^2+z^2\right]\right)\right]$$

  - $Q_n = \frac{y-y_n}{(y-y_n)^2+z^2}$
  - $y_n = \mathrm{nd}$ and d is the array pitch size
  - l is the number of boundary conductors
  - β is the ratio between the boundary and the core conductors currents

Microwave Array with Uniform Magnetic Field

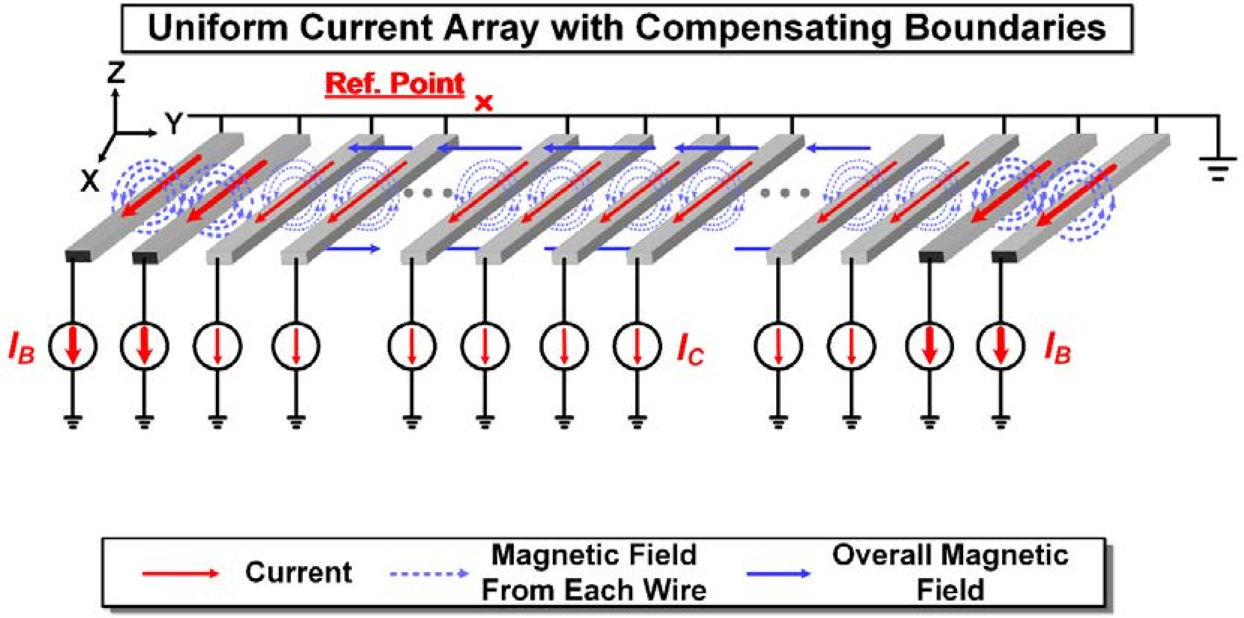

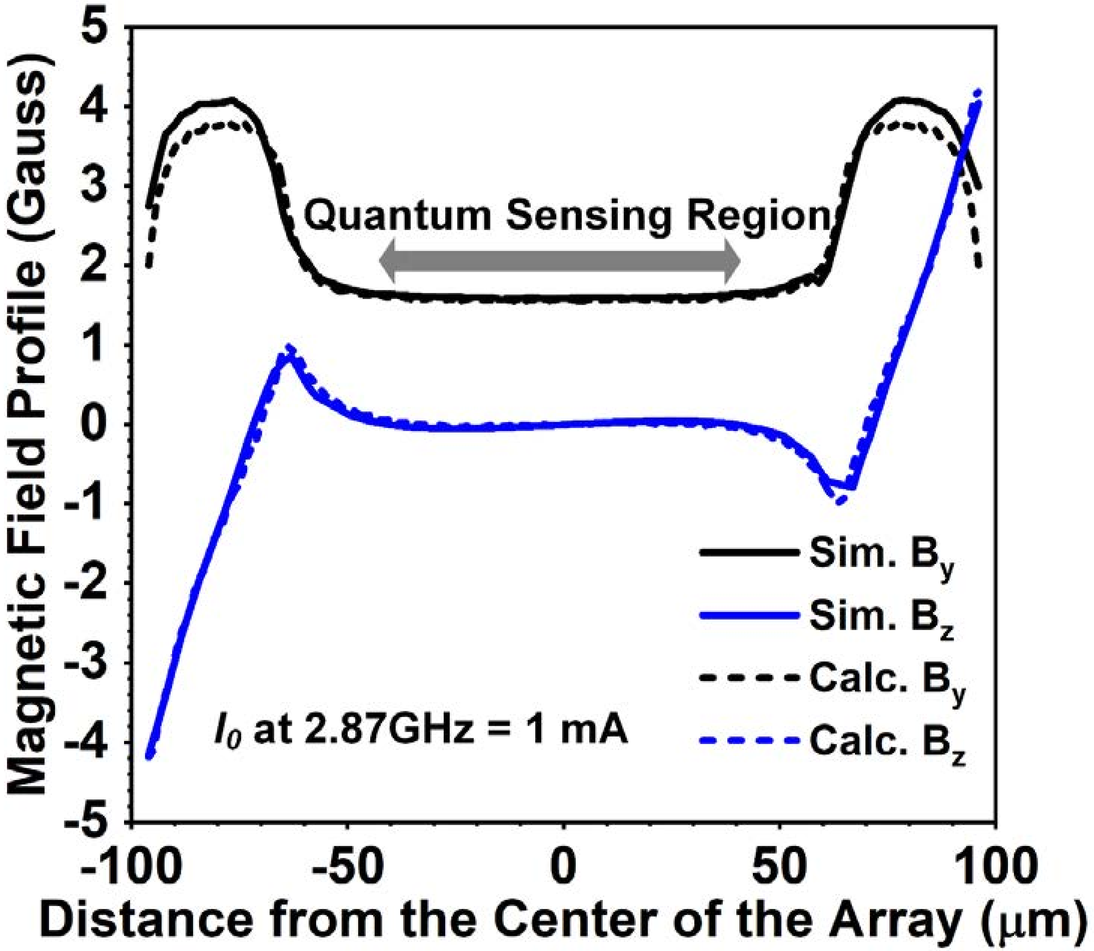

- **Better than 95% uniformity over ~ 50% fill factor is achieved**
- **Non-uniform spacing and current excitation can be investigated**

CMOS Implementation of the Microwave Array

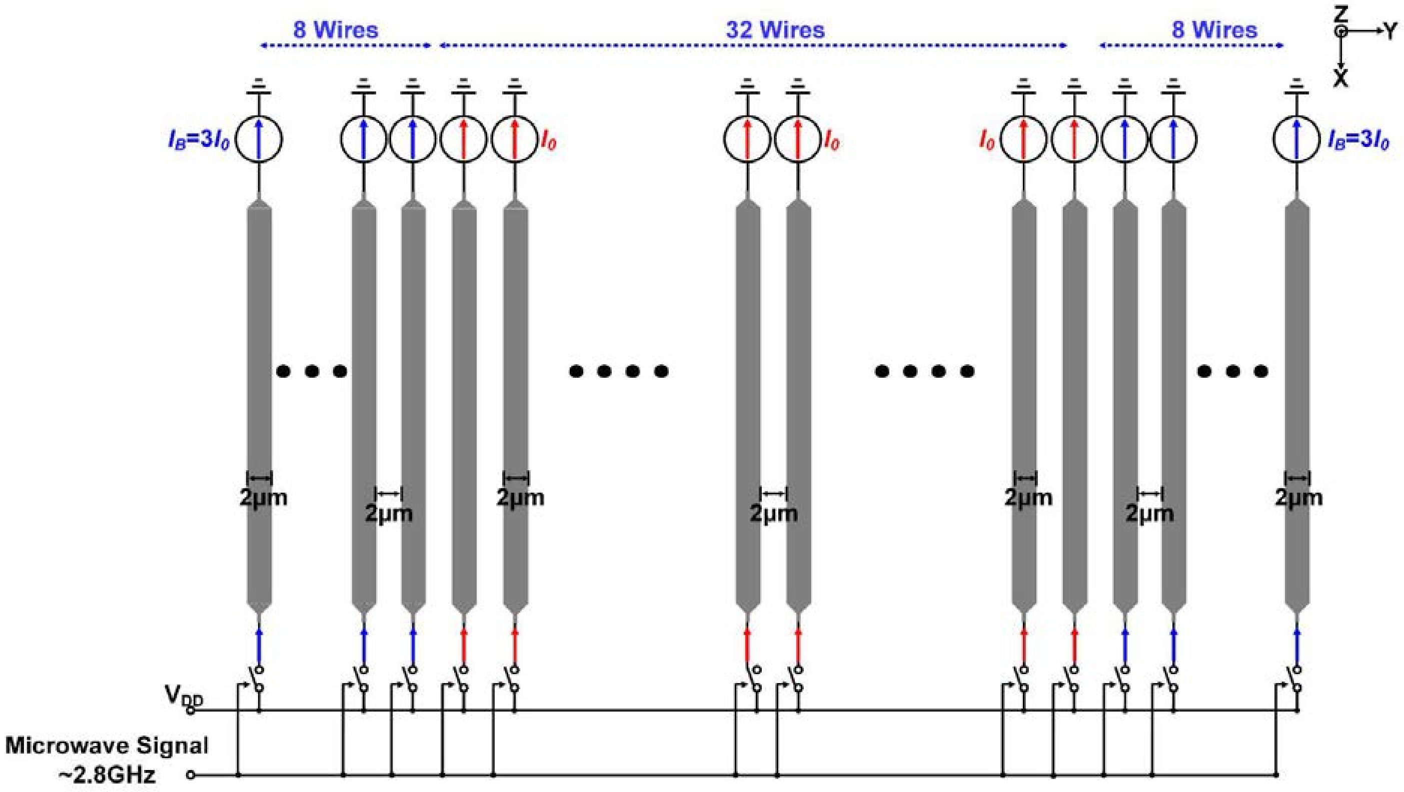

- **The spacing between the conductors is 2μm**
- **The width of the conductors is 2μm**
- **The core current (I_0) is 0.5mA and the boundary current (I_B) is 3I_0**

CMOS Implementation of the Microwave Array

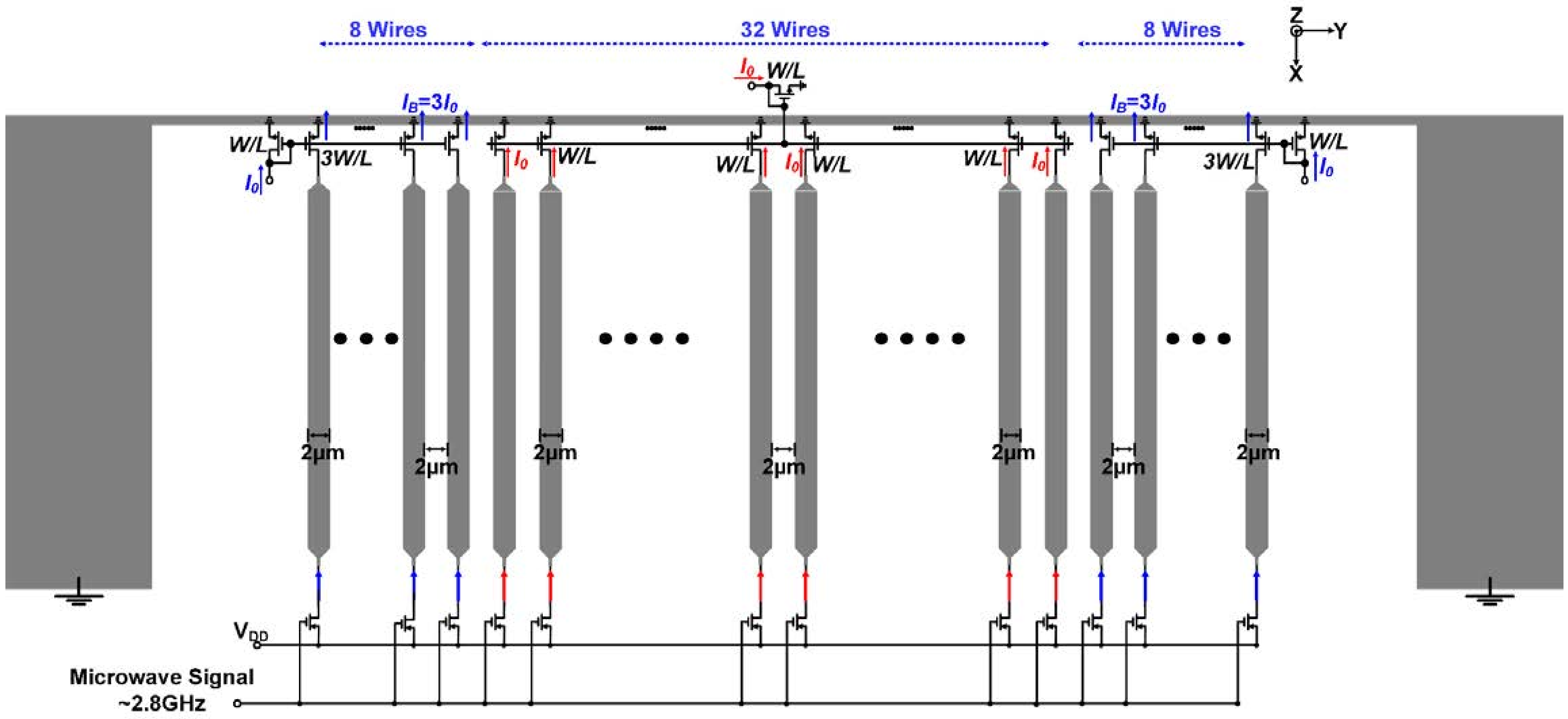

- The spacing between the conductors is 2μm
- The width of the conductors is 2μm
- The core current (I_0) is 0.5mA and the boundary current (I_B) is $3I_0$

© 2019 IEEE

Microwave Generation Circuitry

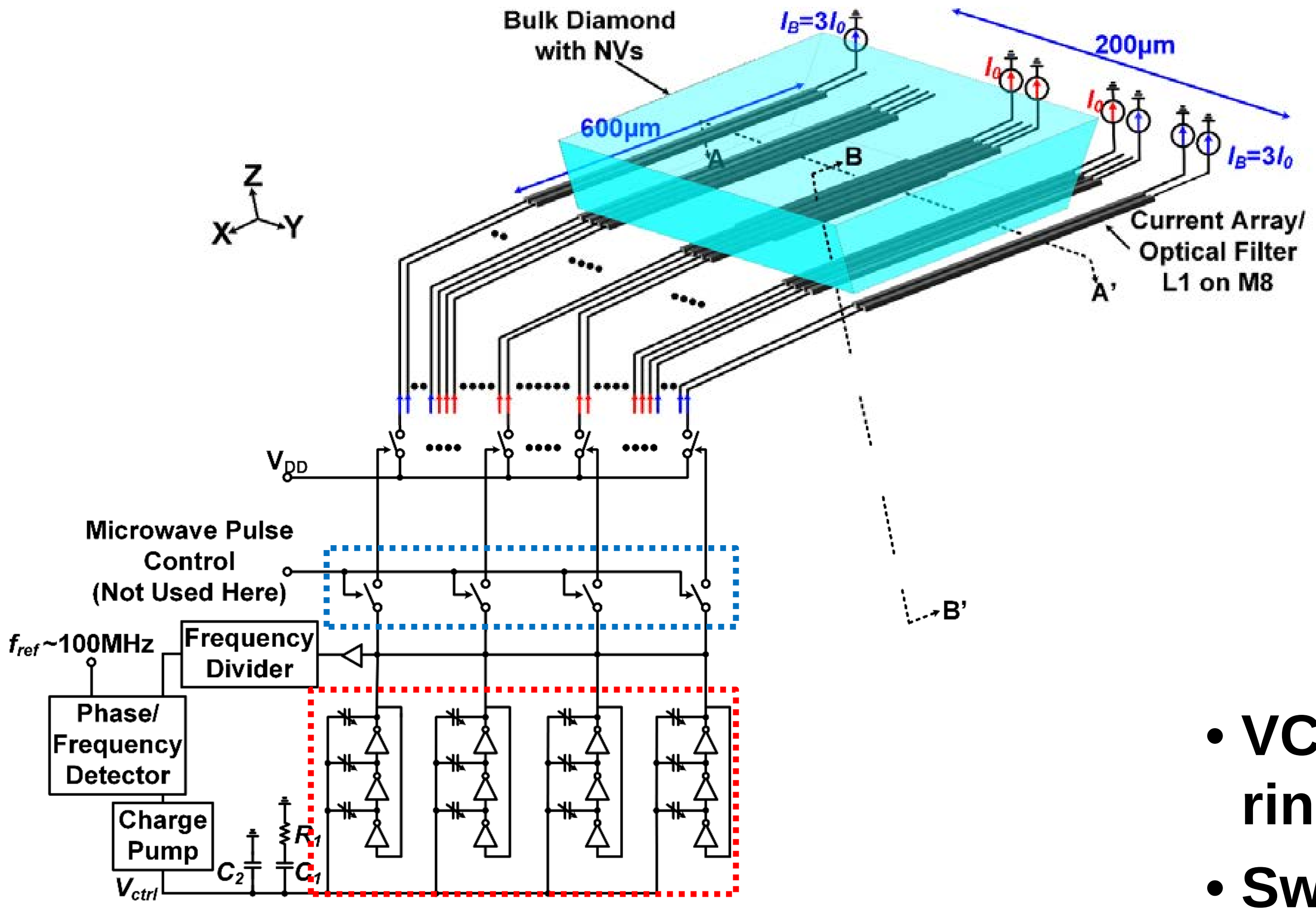

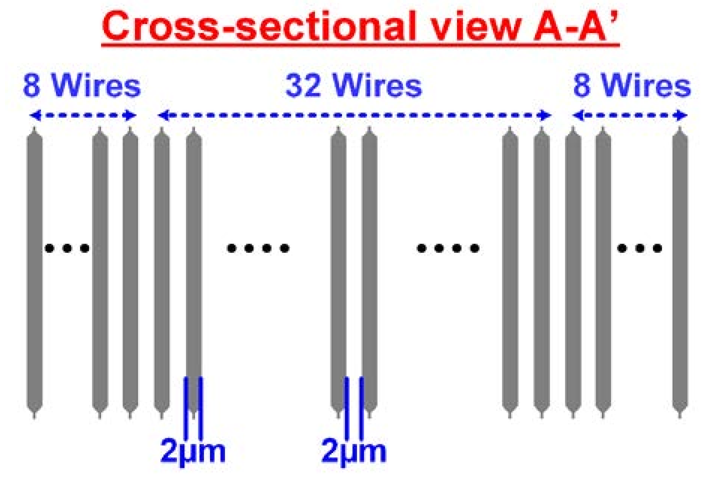

- VCO is based on a bank of coupled ring oscillators
- Switches are added at the output of the PLL to perform pulsed sequences

Optical Excitation Filtering

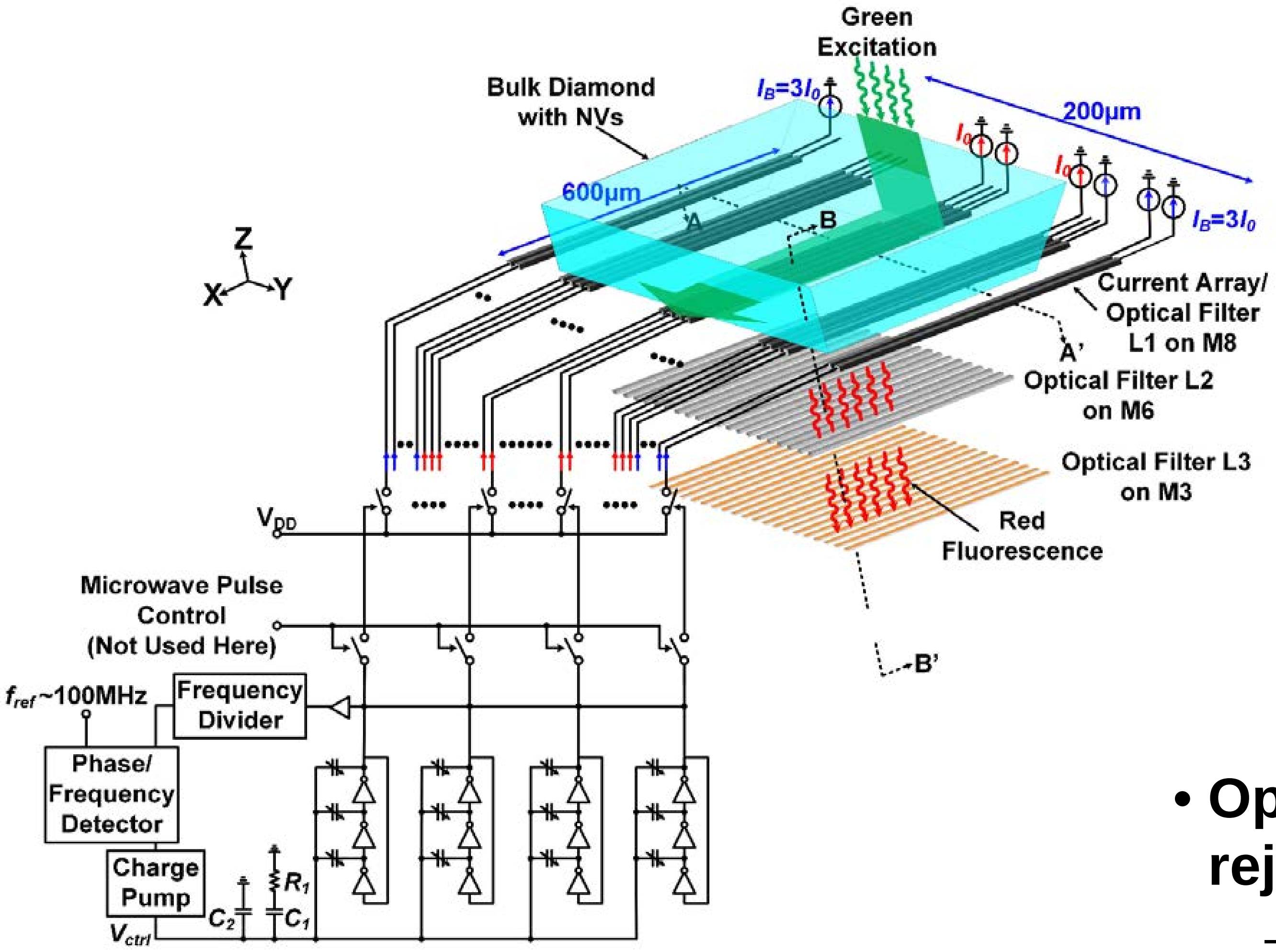

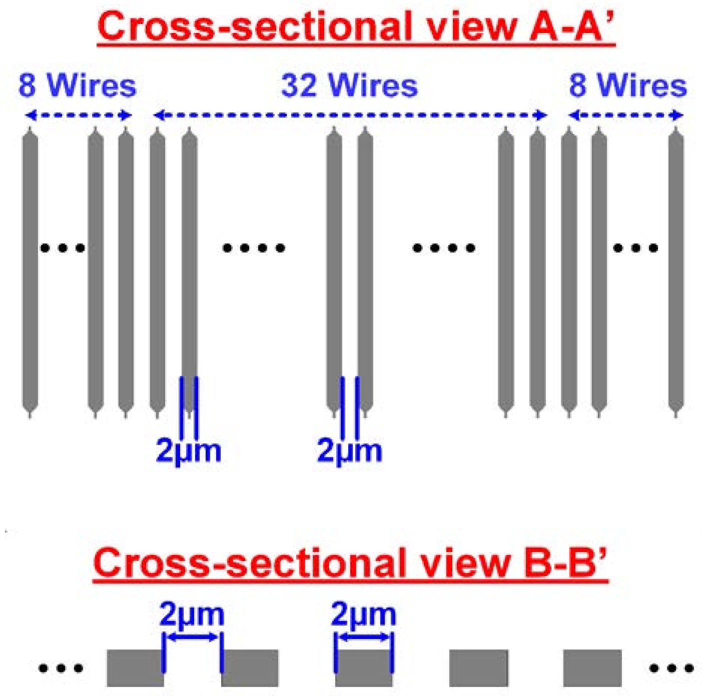

- Optical filtering for green light rejection
  - Decreases the shot noise
  - Increases the contrast

© 2019 IEEE

Optical Excitation Filtering

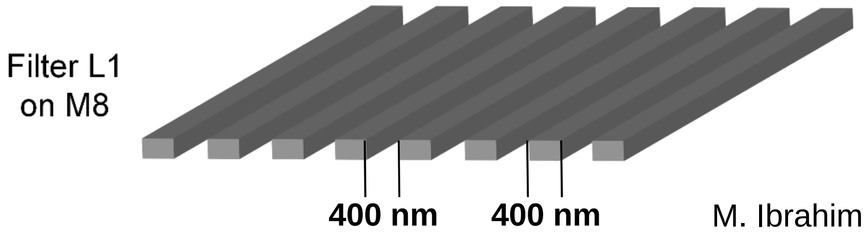

M. Ibrahim, et al., VLSI 2018

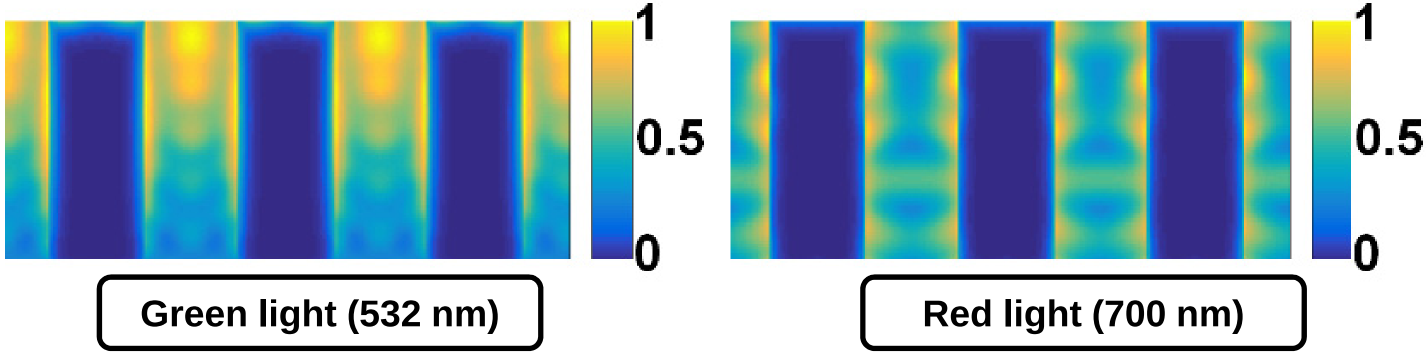

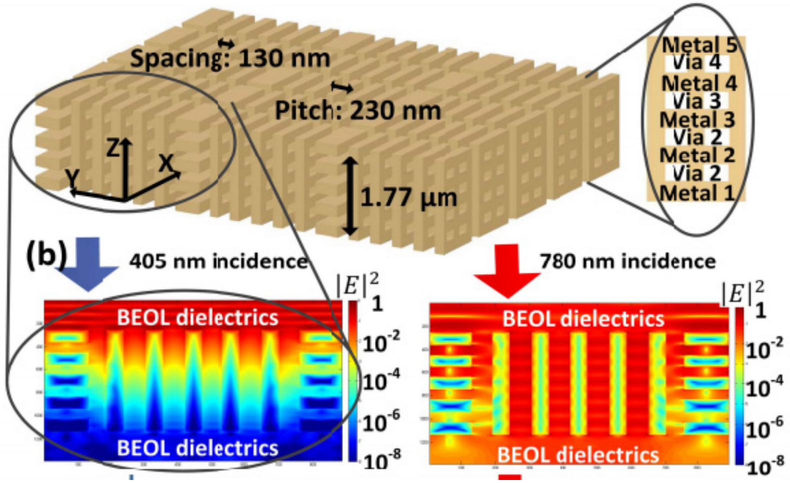

L. Hong, et al., JSSC 2017

- **Previously, we implemented sub-wavelength plasmonic filter**
  - **It is based on wavelength dependent losses**
  - **It is implemented on M8 with measured isolation is 10 dB**
- **Similar filter was used for fluorescence bio-sensing**
- **These filters are enabled by deep sub-µm technology nodes**

Talbot Effect Based Optical Filter Concept

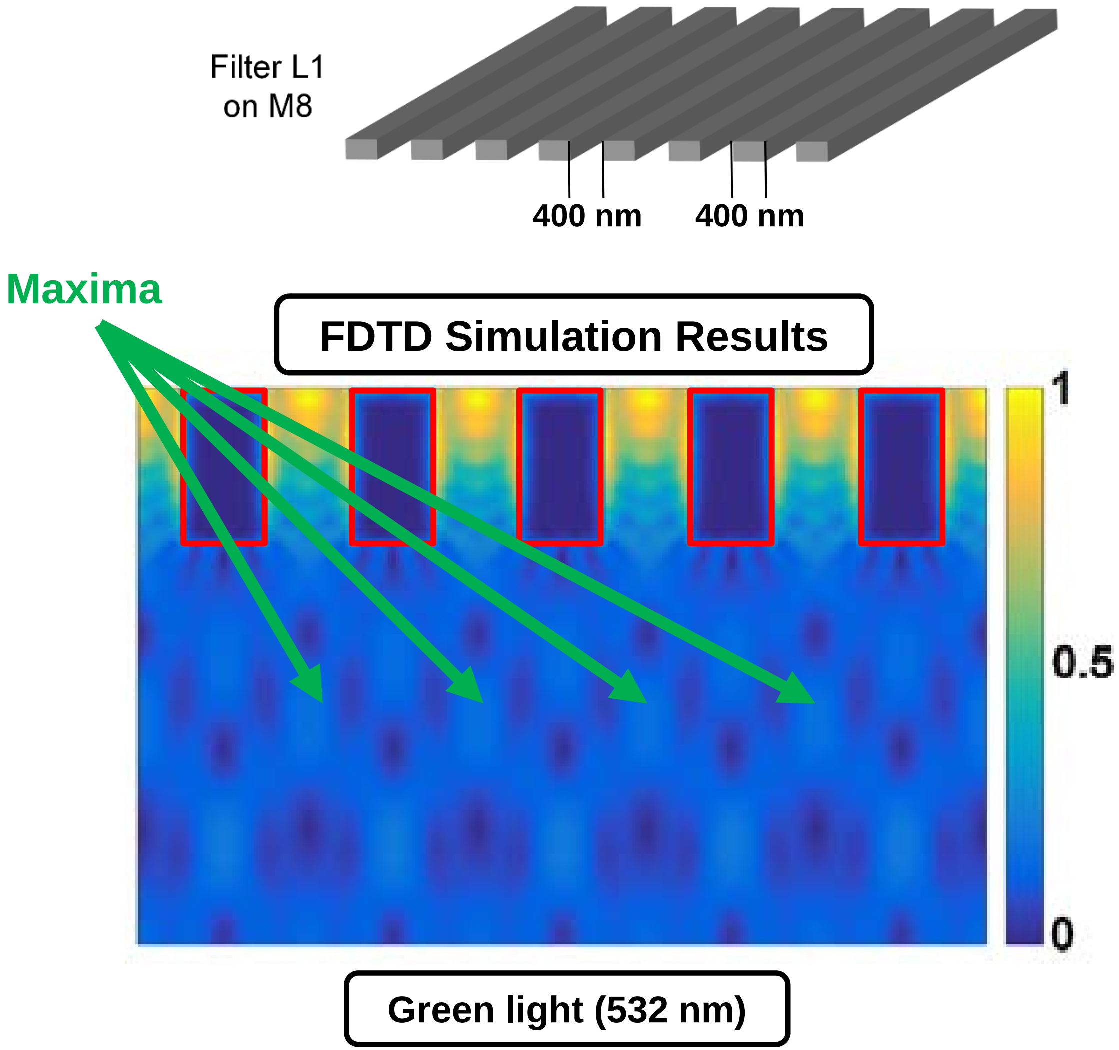

- The grating diffraction pattern form periodic interference patterns
- Second layer is placed at the maxima of the green diffraction pattern
  - Results in extra rejection
- Talbot effect was previously used for angle sensitive camera
  - Transmission depends on the incidence angle at certain wavelength

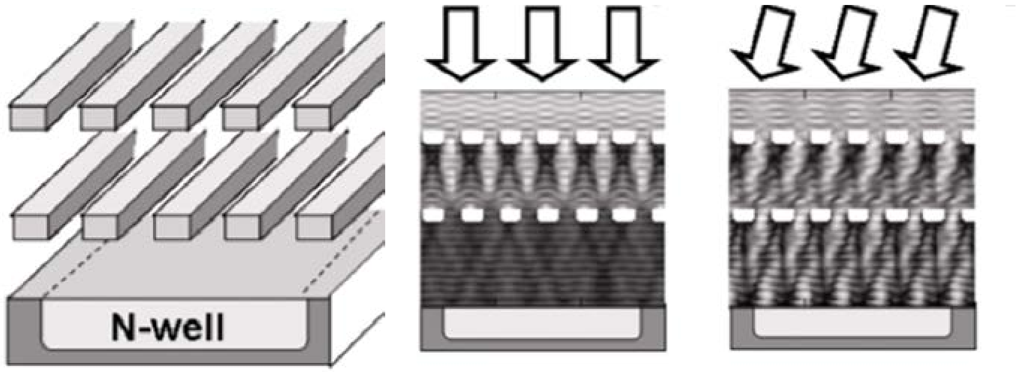

A. Wang, et al., ISSCC 2011

Talbot Effect Based Optical Filter Concept

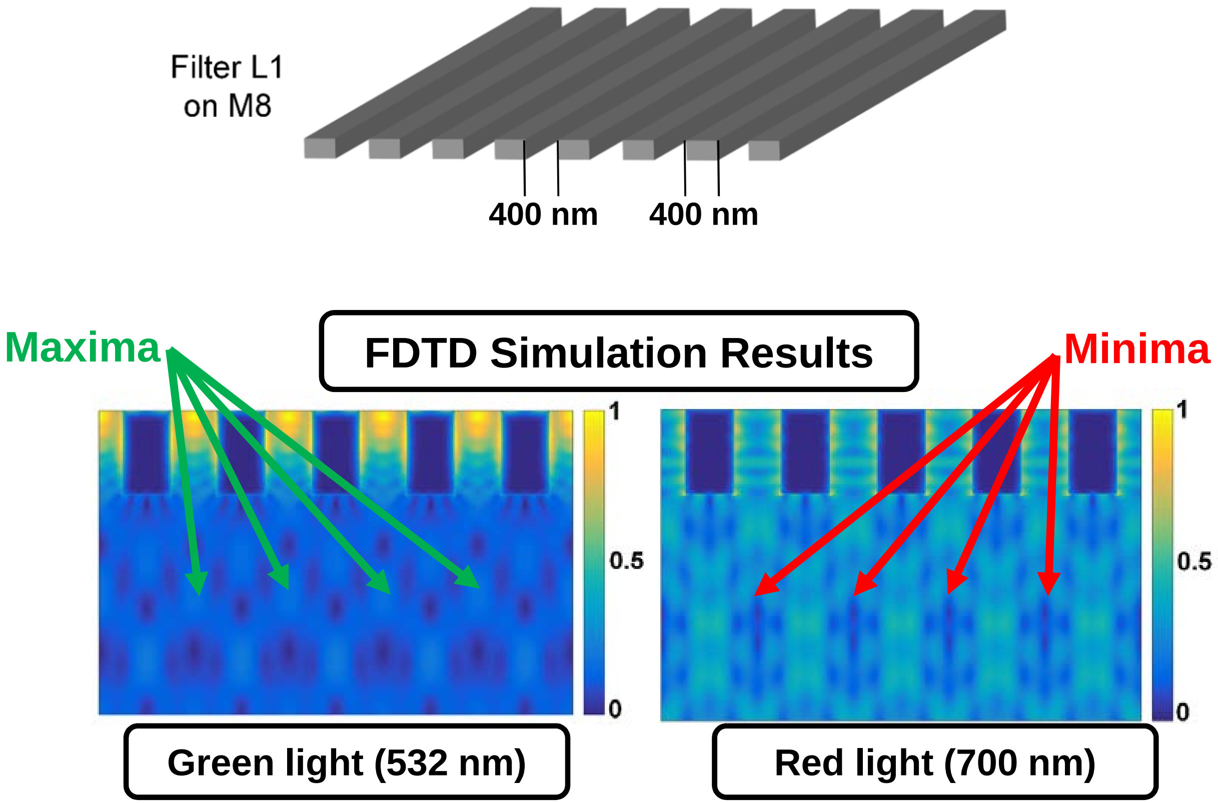

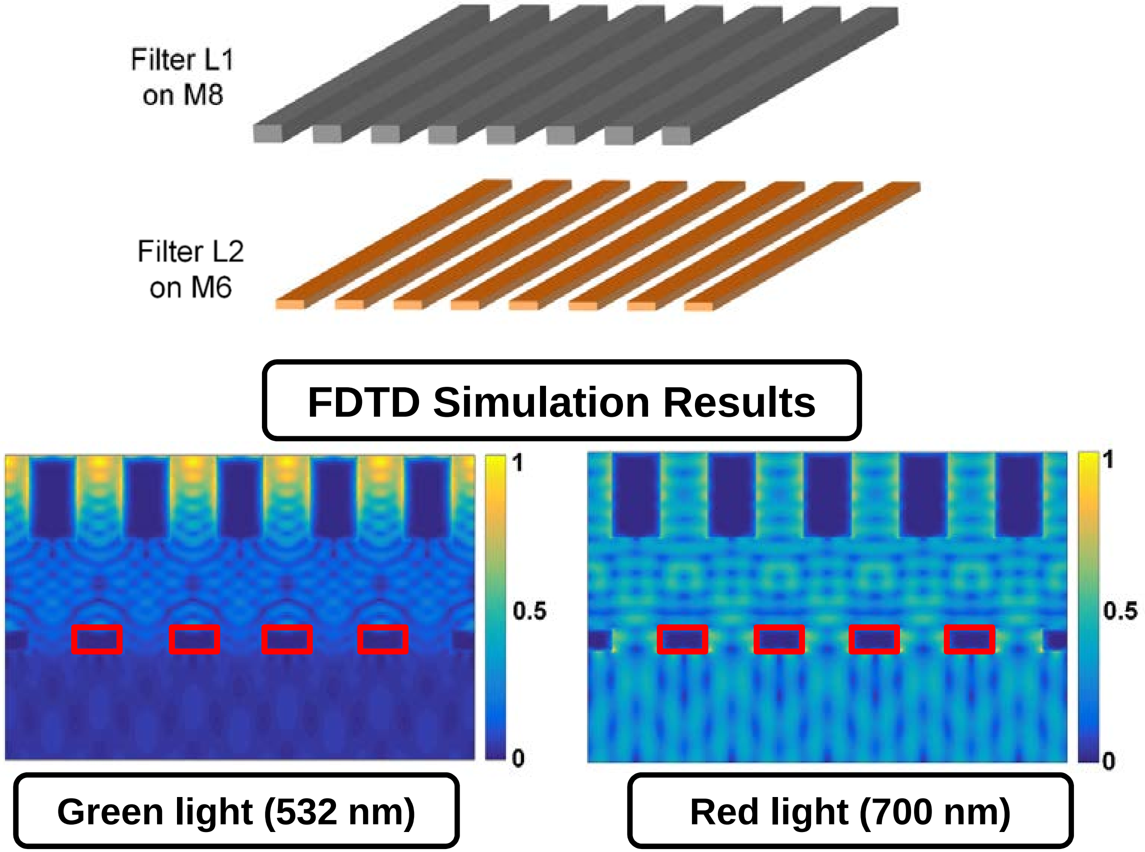

- The second metal layer is placed at M6
- The position is aligned with the maxima of green and minima of red

© 2019 IEEE

Three Layer Optical Filter

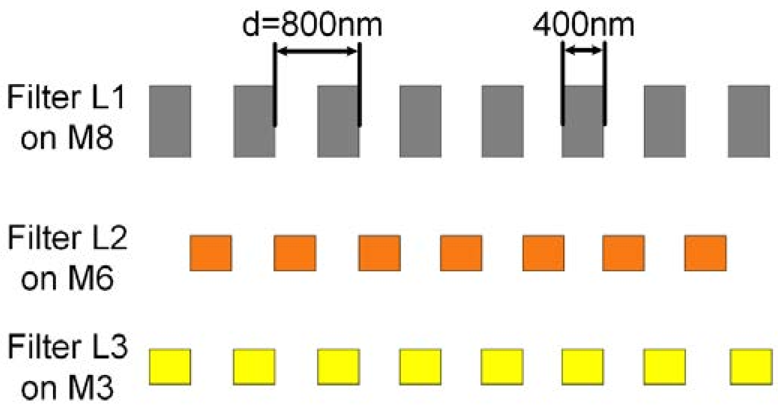

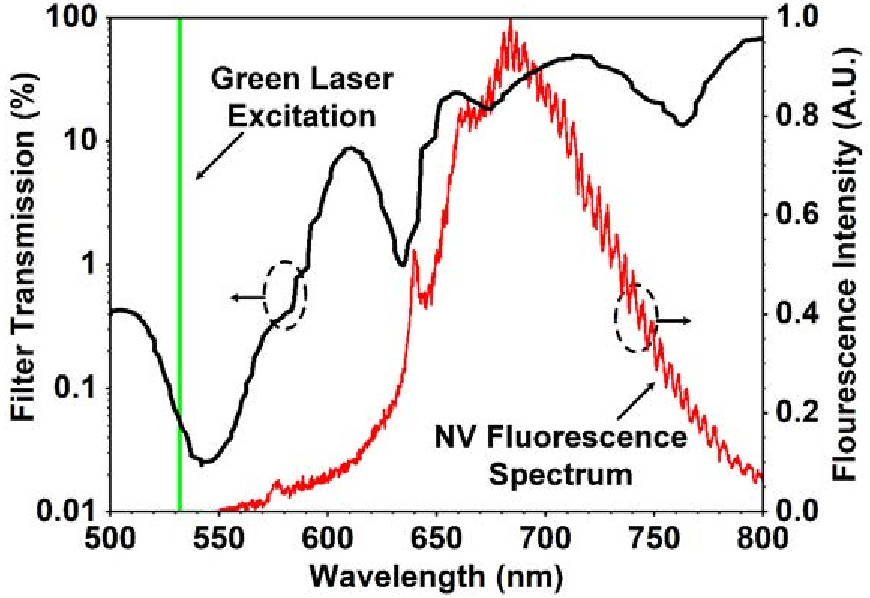

FDTD Simulation Results

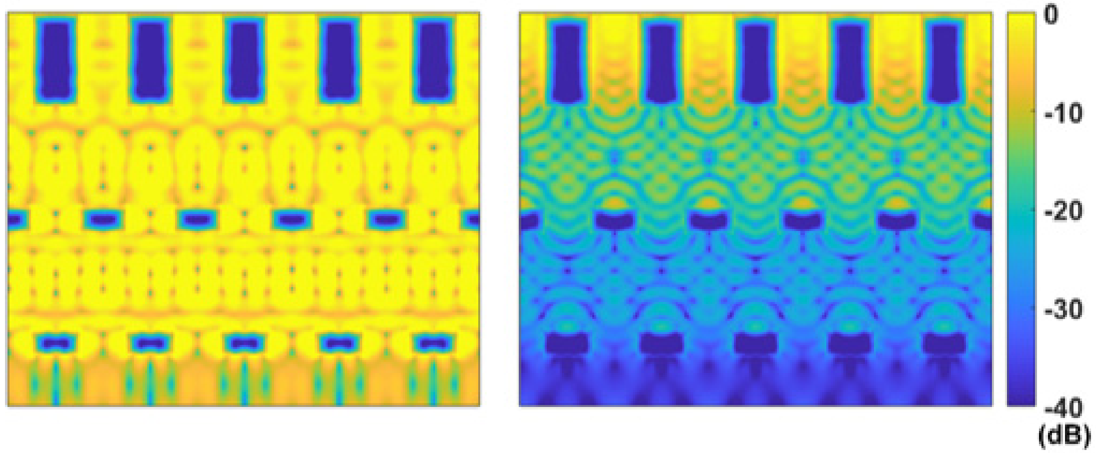

Red light (700 nm)

Green light (532 nm)

- Gratings pitch is 800nm
- Simulated green to red rejection is 30 dB
- Measured isolation for green light is 25 dB

© 2019 IEEE

Microwave Array and Optical Filter Co-Design

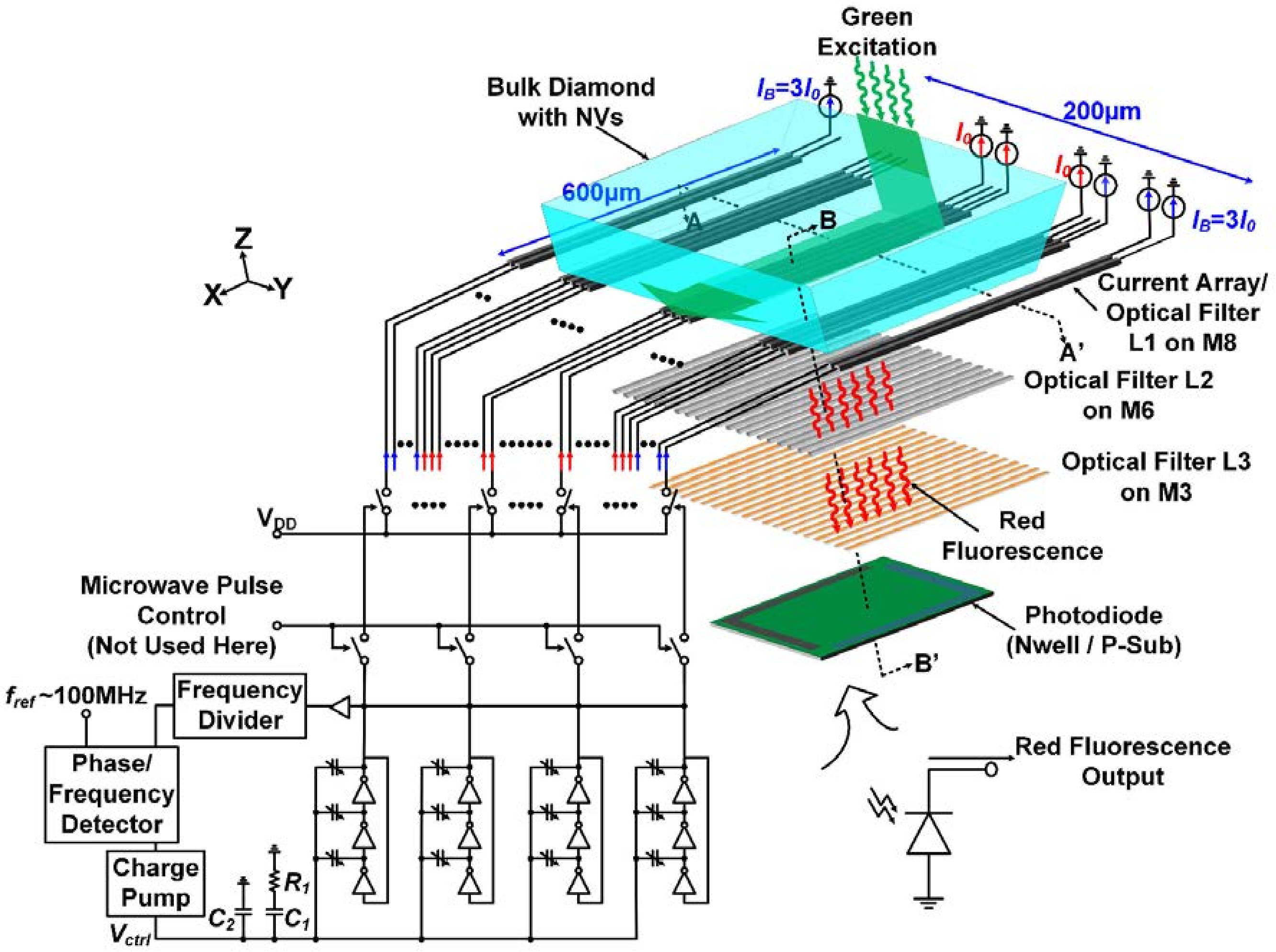

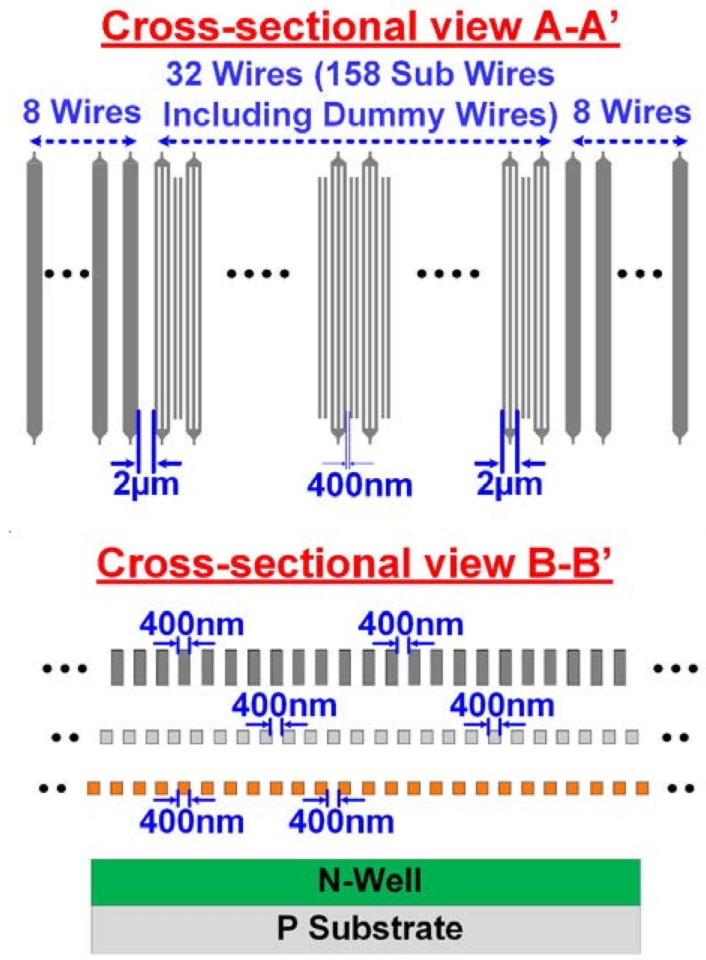

- Measured photodiode responsivity is 180mA/W

© 2019 IEEE

Scalable Hybrid CMOS-Diamond Magnetometer

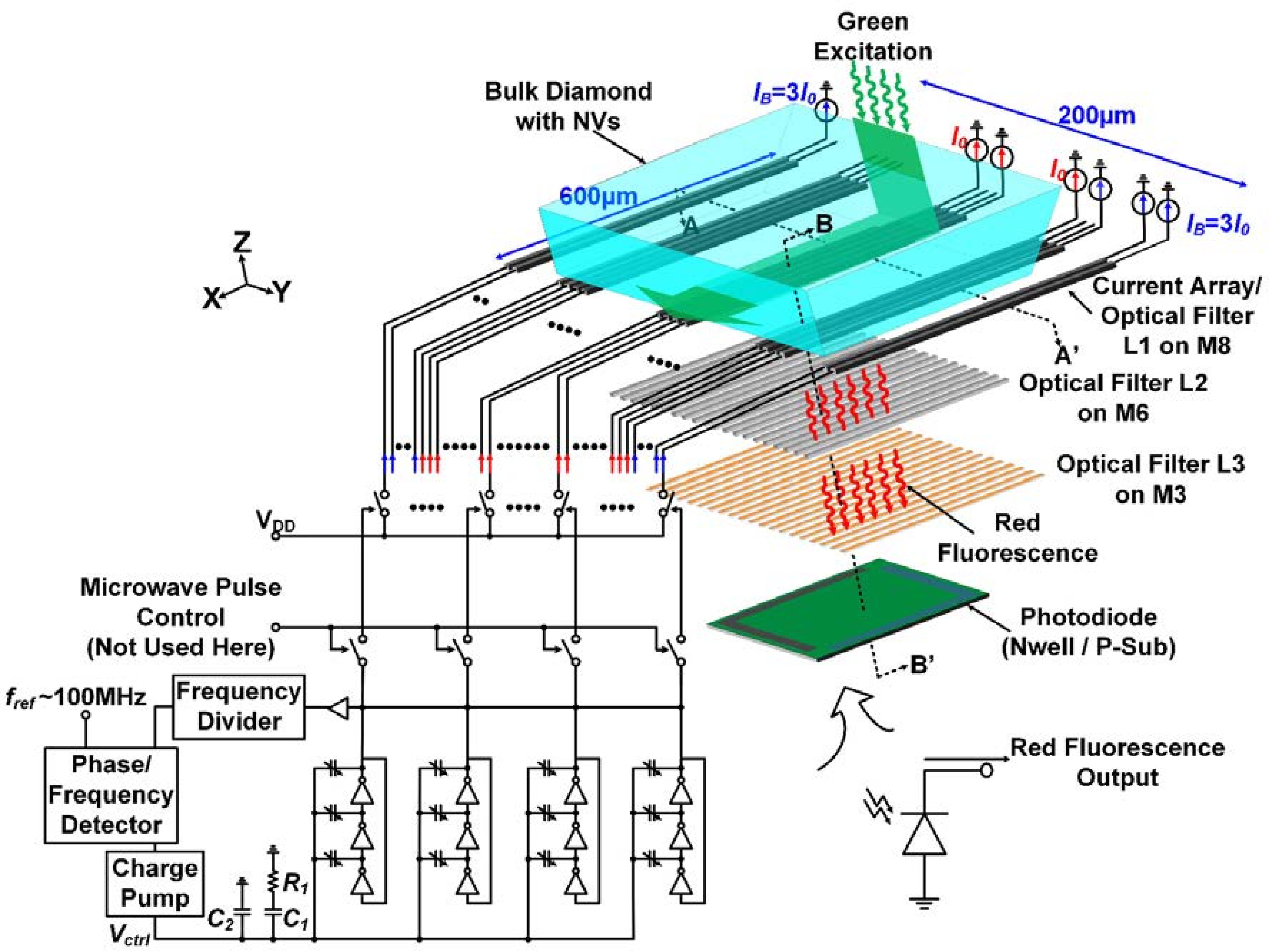

Quantum Sensing Region (Microwave Array, Photonic Filter, and Photodiode)

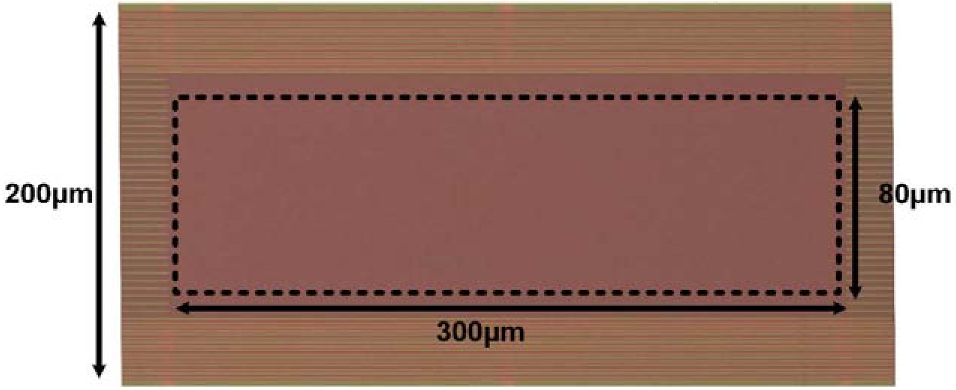

Bulk Diamond with NVs on the Chip

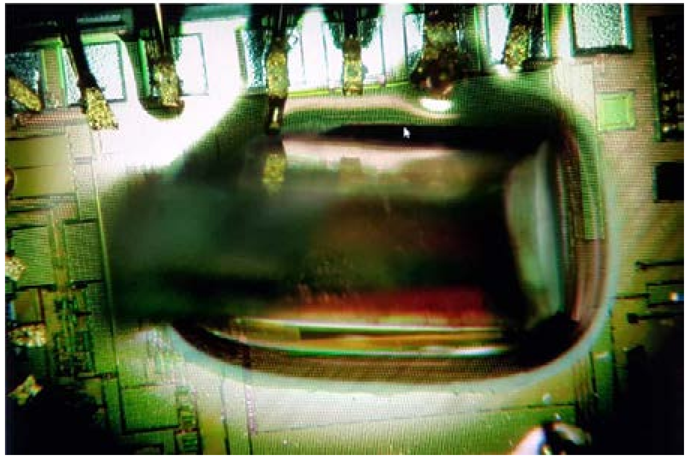

- Diamond is cut to enhance filtering
- Photodiode area is 80µm×300µm

© 2019 IEEE

Outline

- Introduction
- Magnetometry Principle Using NV Centers in Diamond
- Scalable CMOS-Diamond Hybrid Magnetometer
  – Uniform Microwave Array Design
  – Talbot Effect-Based Optical Filter
  – Complete System Integration
- **Measurement Results and Real-Time Demo**
- Conclusions

© 2019 IEEE
International Solid-State Circuits Conference

Chip Micrograph

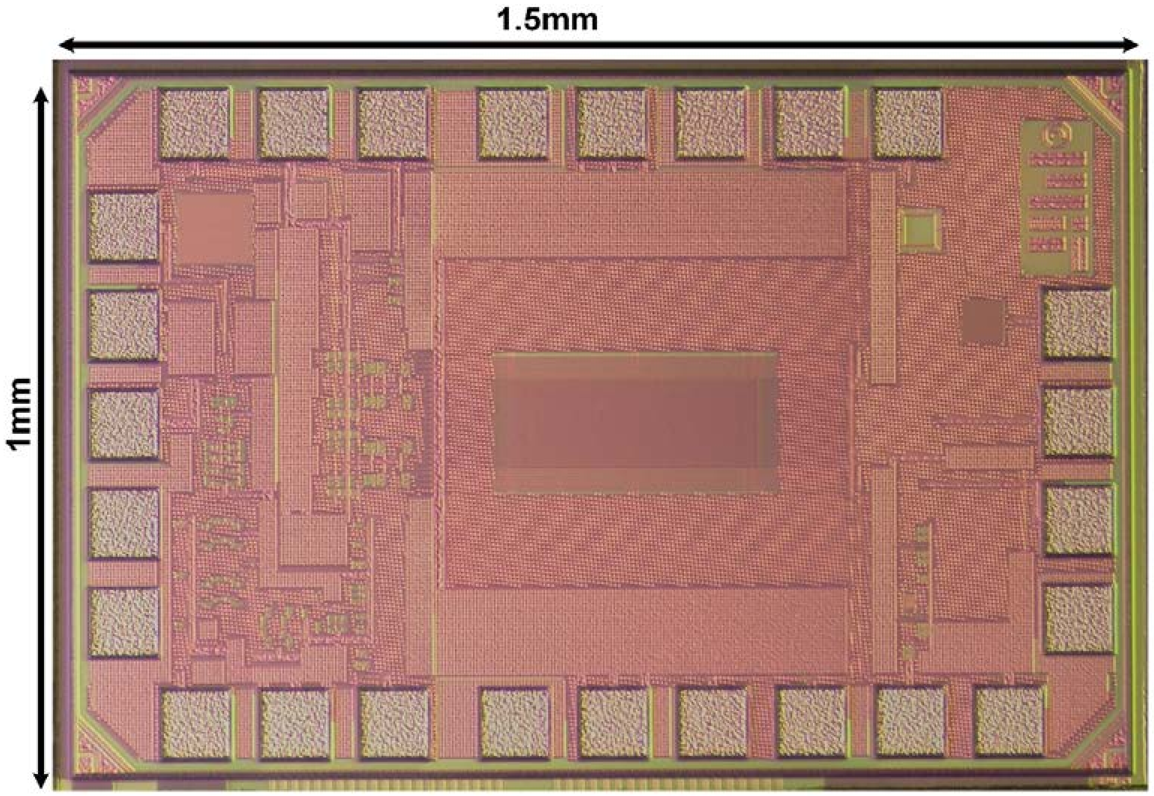

- TSMC 65nm CMOS process
- Chip area: 1mm × 1.5mm
- DC power consumption: 40mW

Measurement Setup

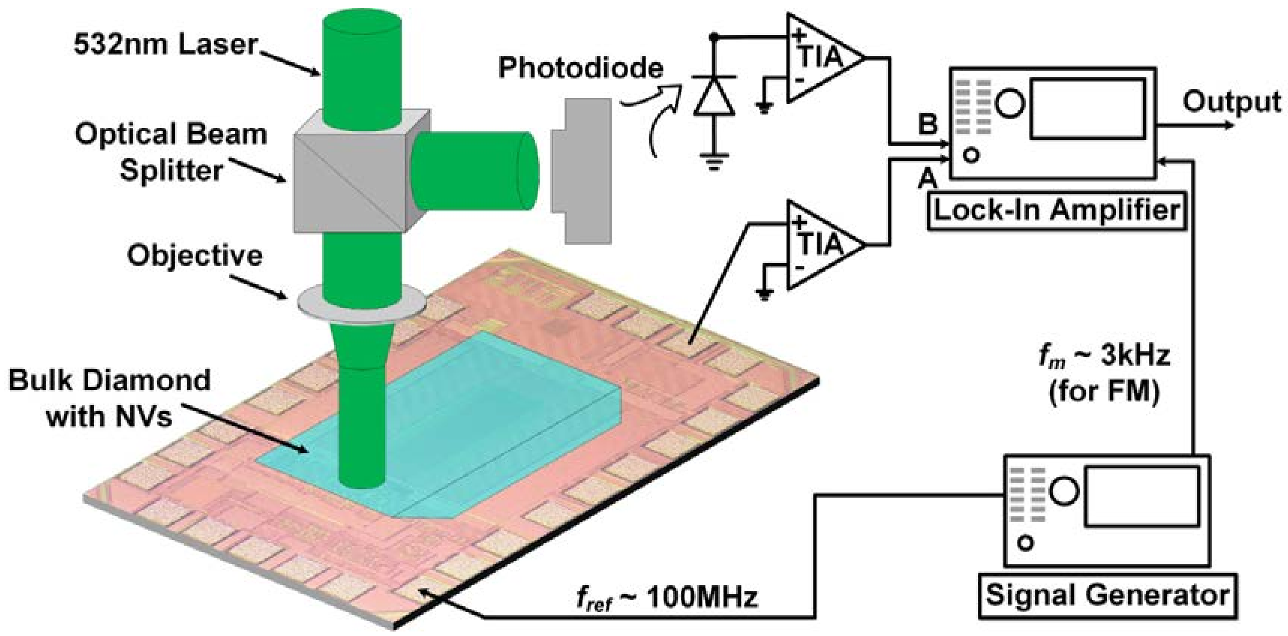

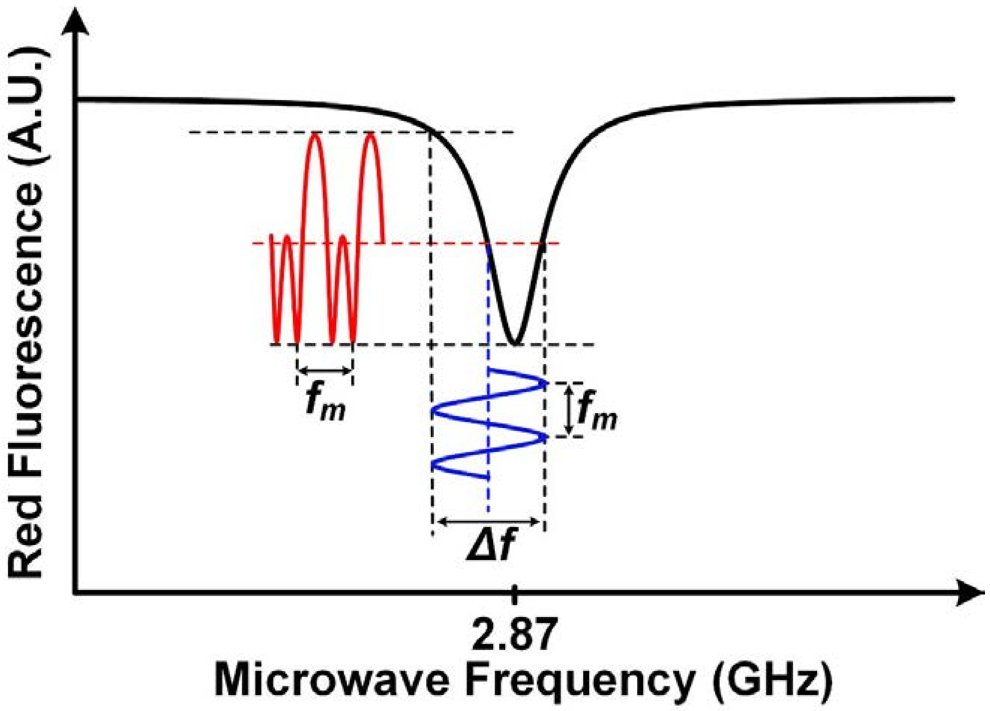

- **Lock-in detection is done to reject the residual unmodulated DC green laser background**
- **Differential measurement is done to cancel the laser intensity variation**

Measured ODMR at Zero External Field

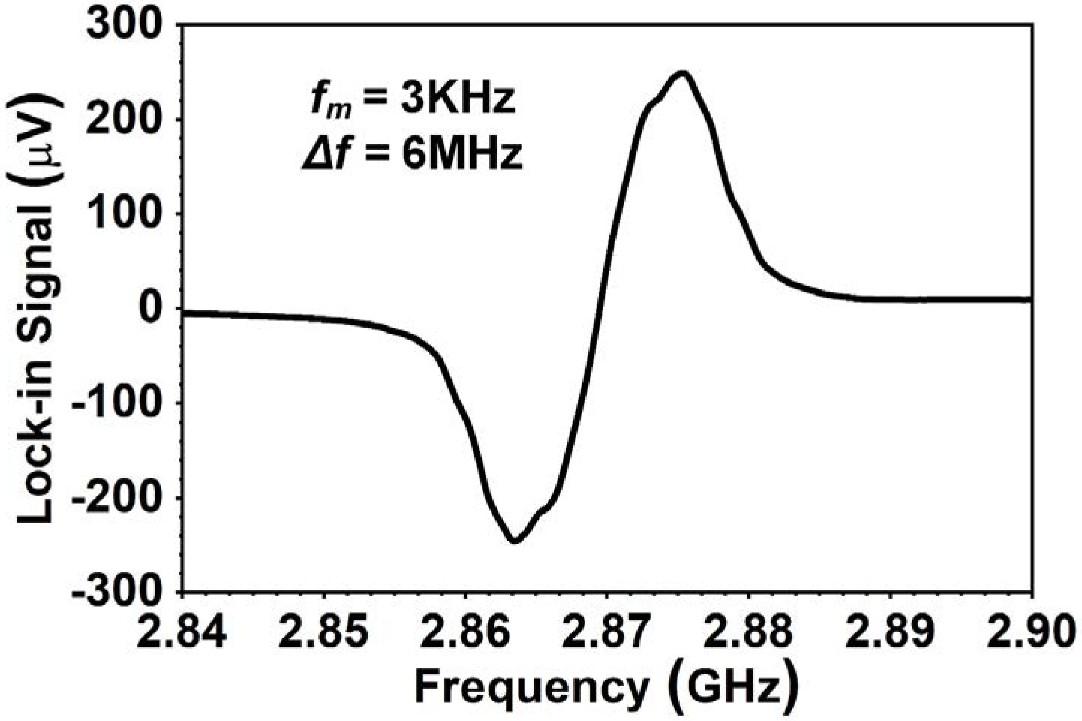

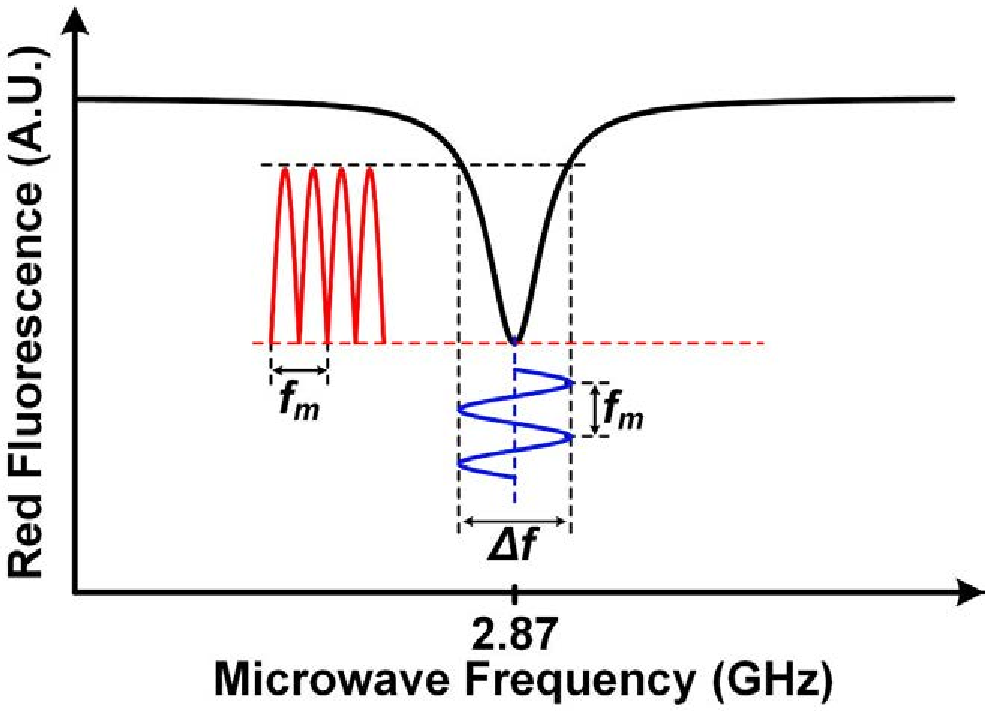

- Wavelength modulated optically detected magnetic resonance (ODMR) at zero external magnetic field is measured
- Wavelength modulation ODMR is close to the derivative of the ODMR without wavelength modulation

Measured ODMR at 5.4mT External Field

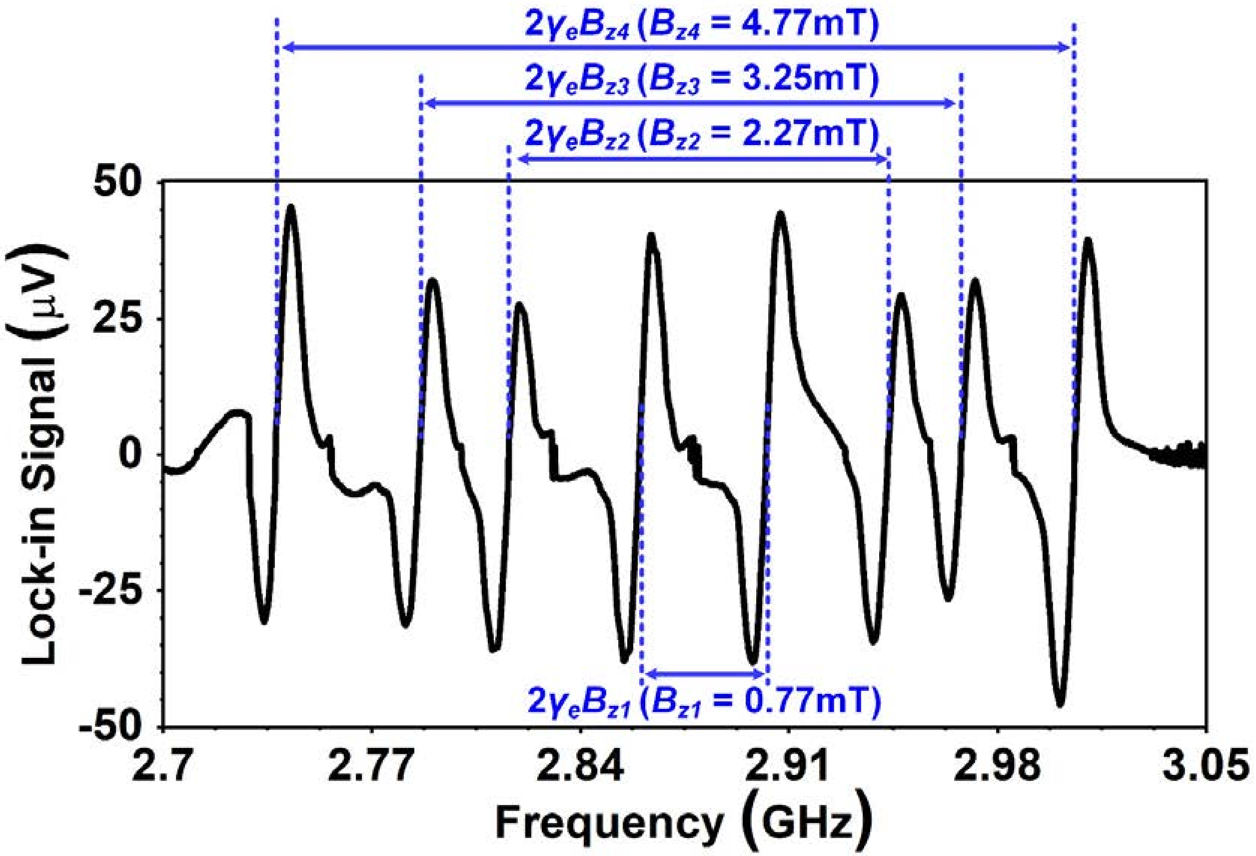

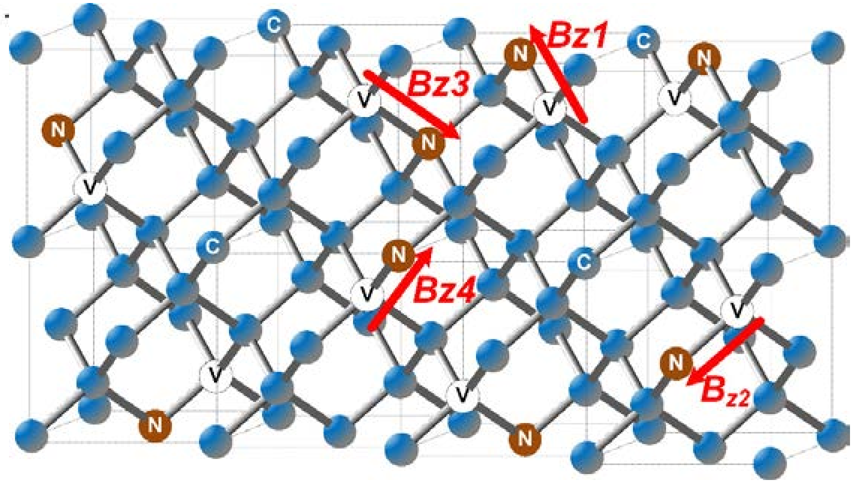

Simulated Conceptual ODMR Curve

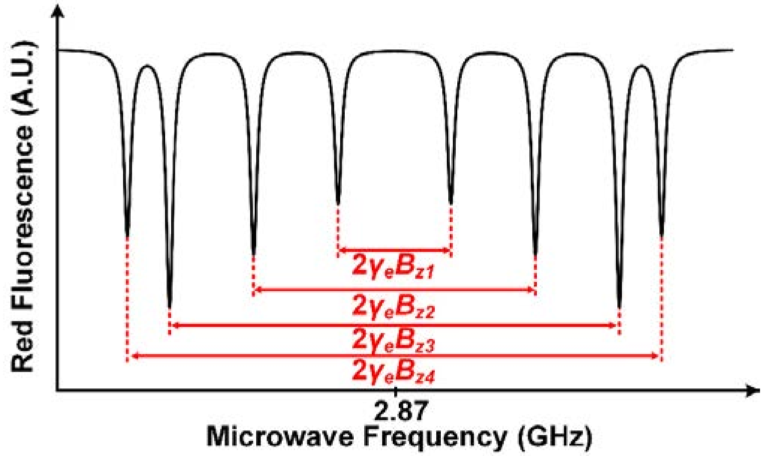

- Permanent DC magnet is applied
- B_{z1}, B_{z2}, B_{z3}, B_{z4} are the projections of B_{ext} along the NV axes

© 2019 IEEE

Magnetic Sensitivity Measurements

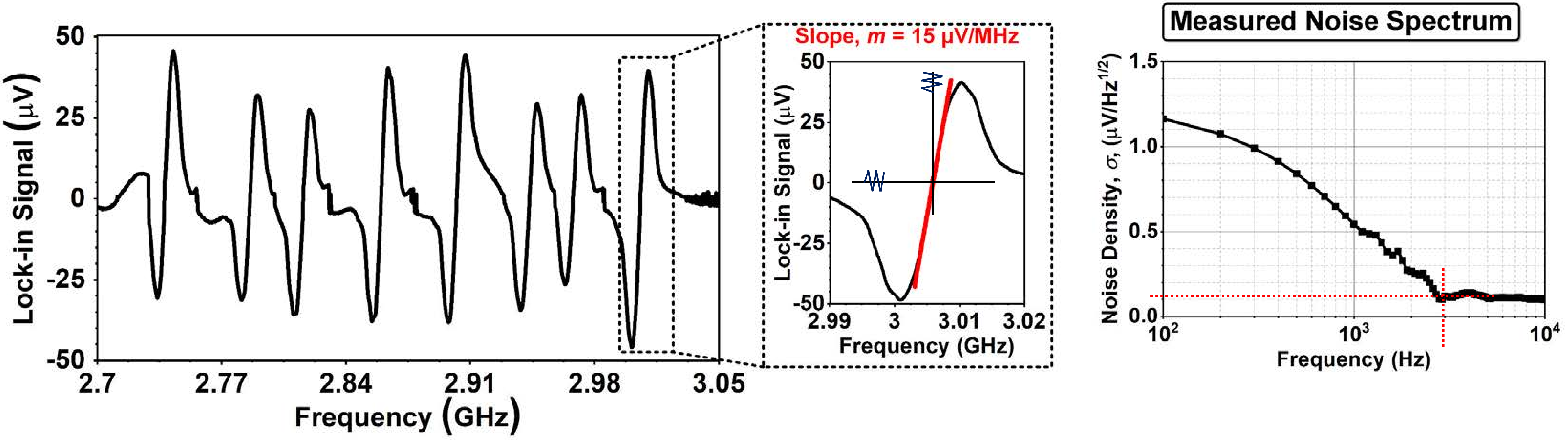

- Magnetic sensitivity is the minimum detectable magnetic field (T/$\sqrt{\text{Hz}}$)
  - Noise voltage, σ = 100nV/Hz$^{1/2}$, Slope, m = 15μV/MHz
  - Gyromagnetic ratio, γ_e= 28 GHz/T
- Magnetic sensitivity, $\eta_{CW} = \sigma/(\gamma_e m)$ = 245nT/$\sqrt{\text{Hz}}$

© 2019 IEEE

Real-Time Vector Field Measurements of a Magnet

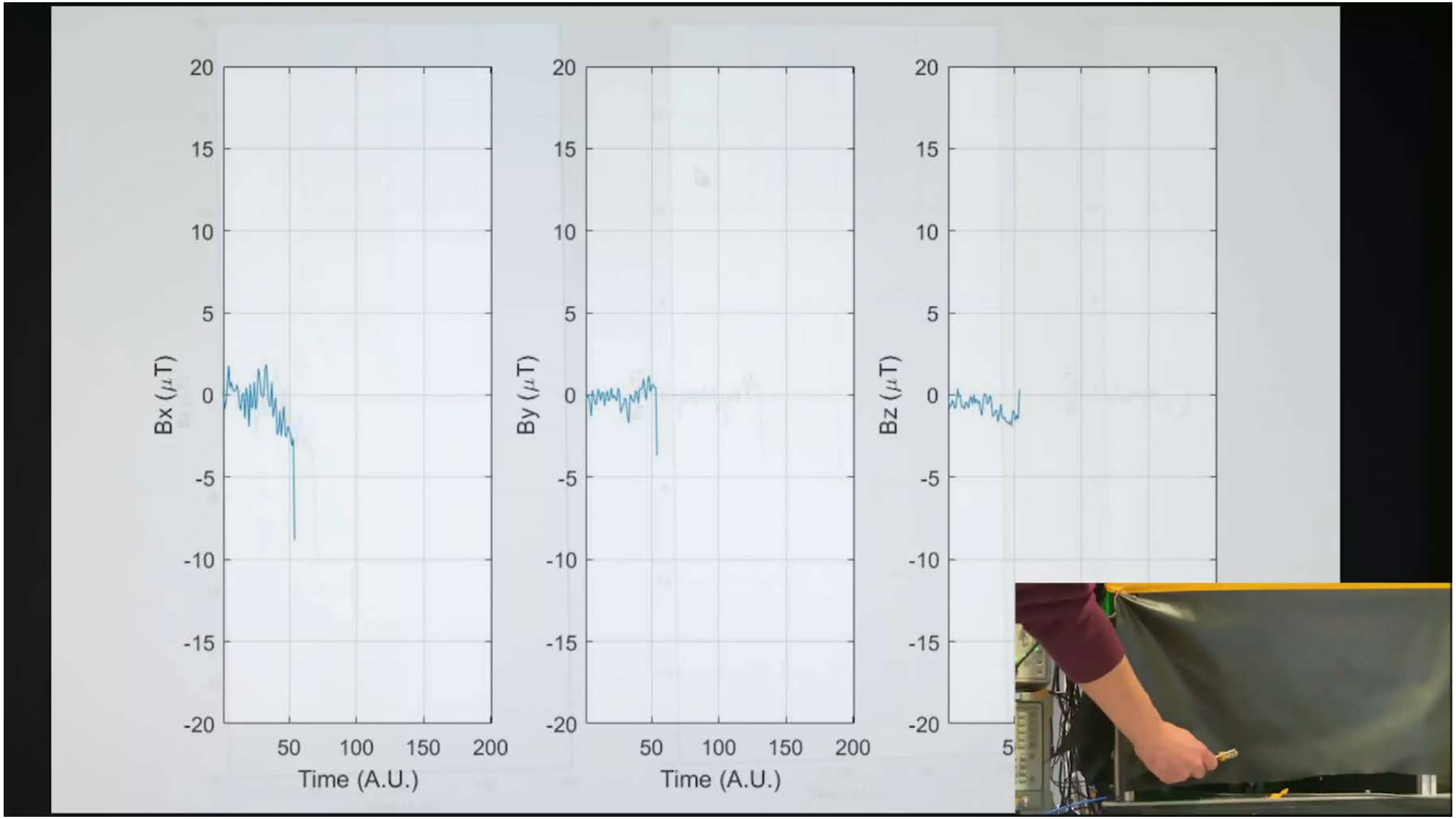

Outline

- Introduction
- Magnetometry Principle Using NV Centers in Diamond
- Scalable CMOS-Diamond Hybrid Magnetometer
  – Uniform Microwave Array Design
  – Talbot Effect-Based Optical Filter
  – Complete System Integration
- Measurement Results and Real-Time Demo
- **Conclusions**

Summary of the Design

- **Hybrid CMOS-Diamond platform for quantum magnetometry**
  - **Combines the advantages of CMOS and NV centers in diamond**
  - **Enables a compact sensitive magnetic field sensor**
- **Co-designed scalable microwave coupling structure and photonic filter**
  - **Can be scaled to larger areas for better sensitivity**
  - **Offers high isolation filtering on CMOS**
- **Coherent control of NV ensembles**
  - **Enables the implementation of advanced spin control sequences**
- **Integrated system that perform spin state coherent control and readout**
  - **Offers closed-loop feedback between spin-manipulation and readout**
  - **Decreases the number of IOs**

CMOS-Diamond Scalable Magnetometer

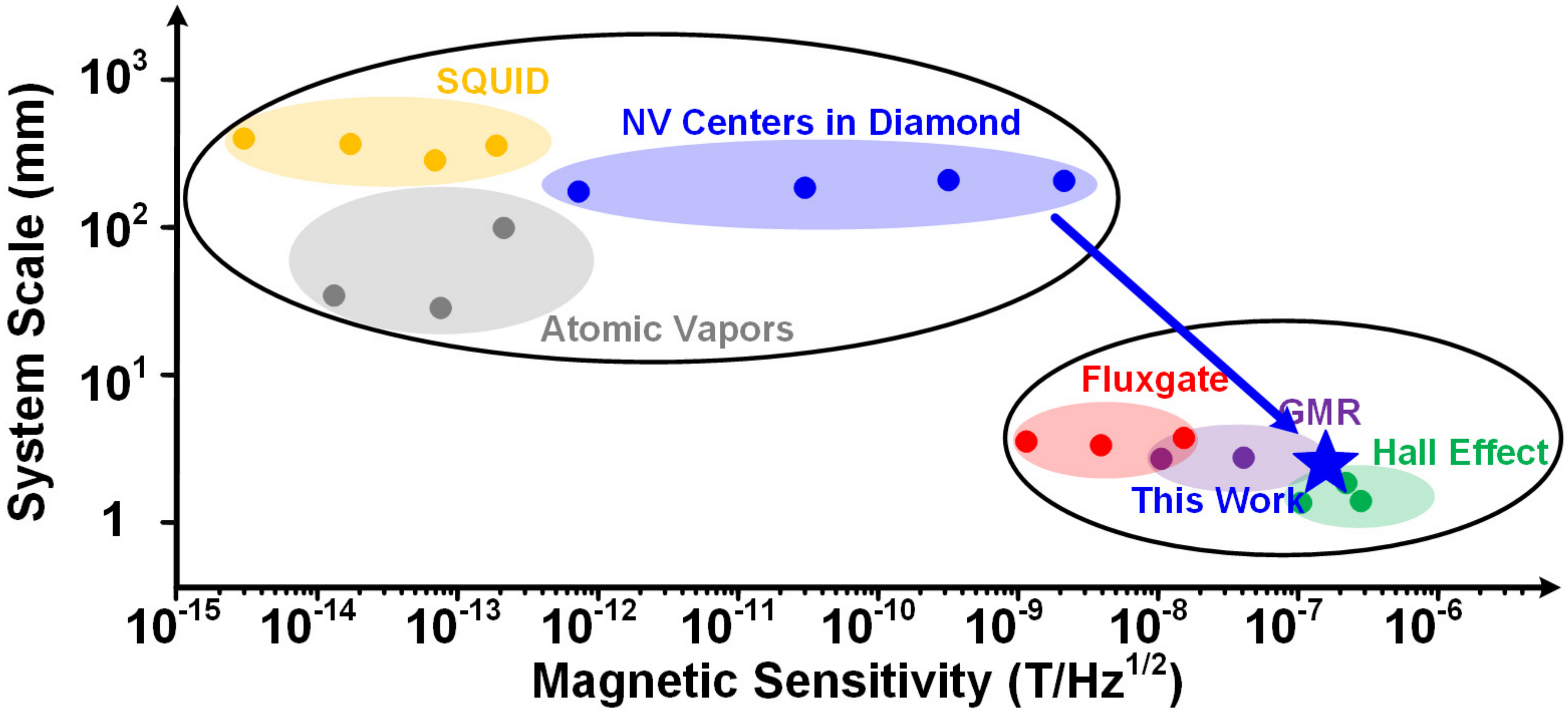

© 2019 IEEE

CMOS-Diamond Magnetometer Sensitivity Roadmap

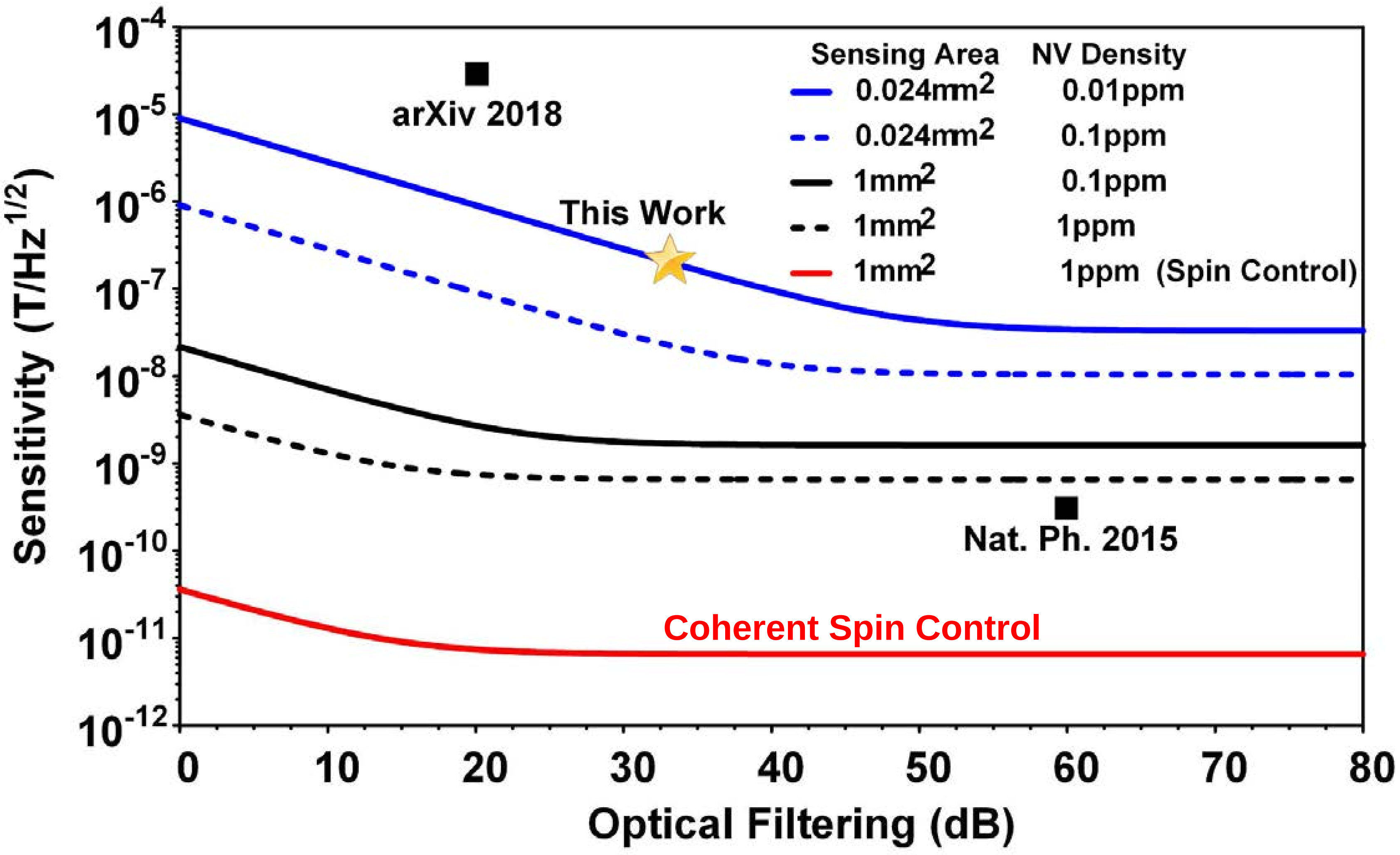

The Future of CMOS-Diamond Magnetometer

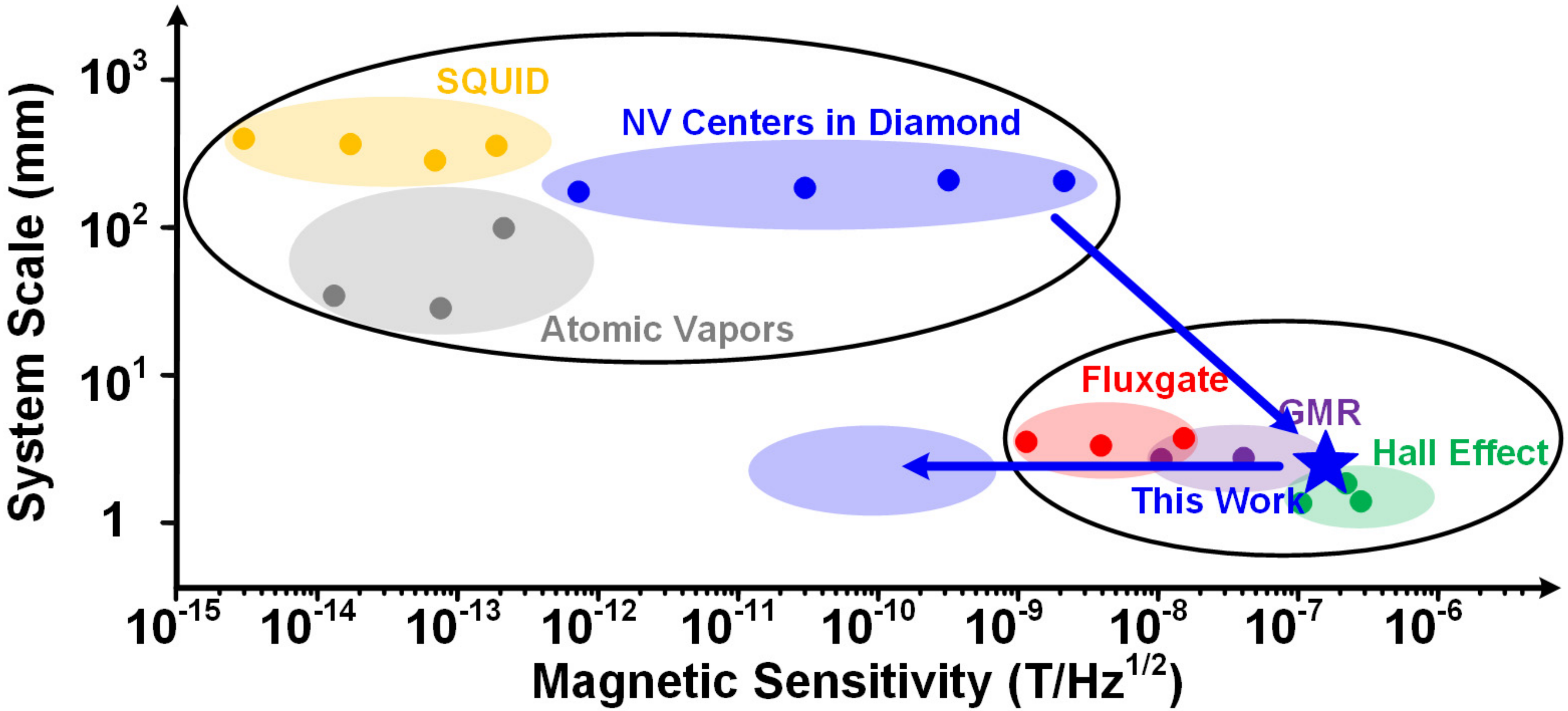

© 2019 IEEE

The Future of CMOS-Diamond Quantum Sensing

- **Integrated CMOS-Diamond platforms that can be used for magnetic field imaging or distributed sensing**

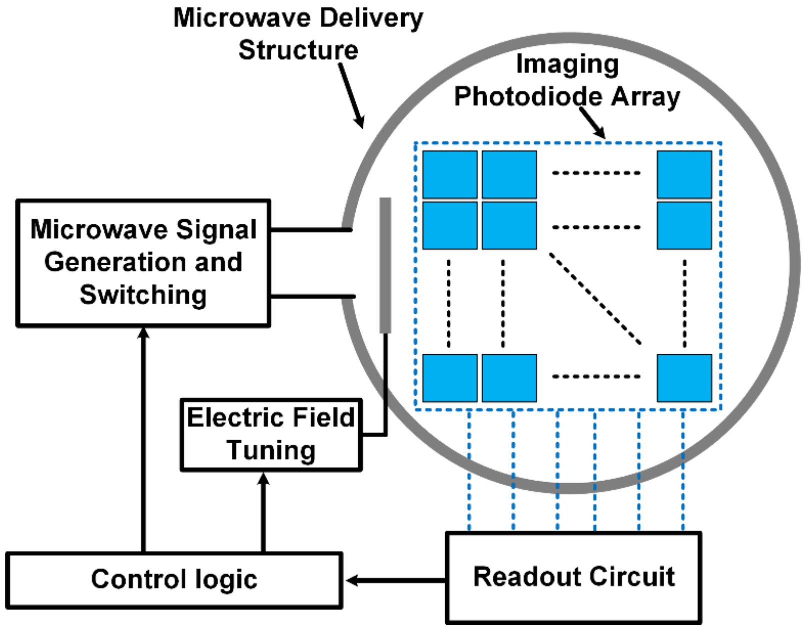

Imaging Platform

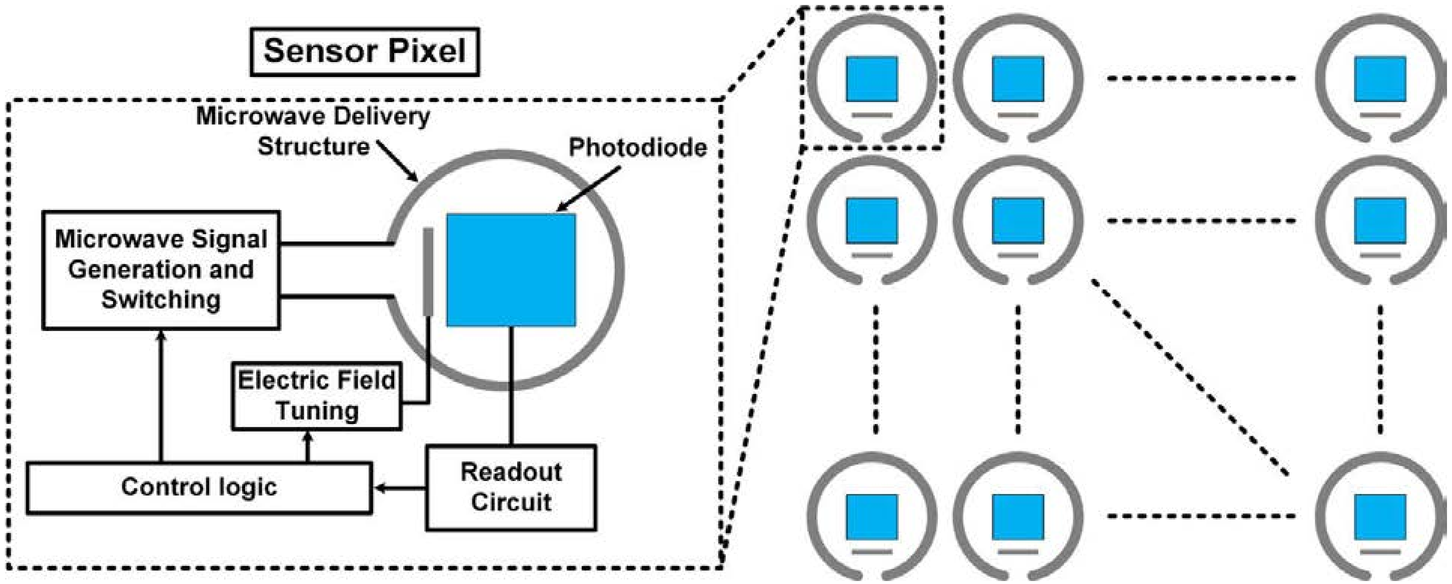

Distributed/Parallel Sensing Platform

© 2019 IEEE

Acknowledgement

- National Science Foundation (RAISE-TAQS: 1824360)
- MIT Center for Integrated Circuits & Systems
- Singaporean-MIT Research Alliance
- Master Dynamic Limited
- Army Research Office MURI on “Imaging and Control of Biological Transduction using NV-Diamond”
- Xiang Yi, Donggyu Kim, David Bono, and Cheng Peng at MIT for their technical assistance during prototyping and testing